Plant Soil (2020) 449:209–231
https://doi.org/10.1007/s11104-020-04465-9

REGULAR ARTICLE

Hydrogen sulfide is a crucial element of the antioxidant defense system in *Glycine max–Sinorhizobium fredii* symbiotic root nodules

Hang Zou · Ni-Na Zhang · Xue-Yuan Lin · Wei-Qin Zhang · Jian-Hua Zhang · Juan Chen · Ge-Hong Wei

Received: 26 August 2019 / Accepted: 19 February 2020 / Published online: 11 March 2020

Abstract

Aim H_2S is emerging as a signaling molecule involved in the regulation of many physiological processes in plants. Here, we investigated the potential antioxidant role of H_2S in soybean (*Glycine max*)-rhizobia (*Sinorhizobium fredii*) symbiotic root nodules.

Method An endogenous H_2S production deficit rhizobia mutant Δ*CSE* was constructed to study the effect of decreased content of H_2S in soybean nodules. Fluorescent probes and confocal microscope were used to observe the production and accumulation of H_2S and reactive oxygen species. Transmission electronic microscopy was conducted to study the structural changes in Δ*CSE* soybean nodules. Finally, qRT-PCR, enzymatic activity, and oxidative damage parameters were measured.

Result The results demonstrated that abundant H_2S was generated in the nitrogen-fixing zone of soybean nodules. The deletion of the cystathionine γ-lyase (*CSE*) gene in *S. fredii* (Δ*CSE*) caused a sharp decrease in H_2S production in both free-living rhizobia and soybean nodules. We found that decrease in the H_2S level in nodule cells inhibited nitrogenase activity. In addition, to elevated H_2O_2 and malondialdehyde accumulation,

Hang Zou and Ni-Na Zhang contributed equally to this work.

Responsible Editor: Ulrike Mathesius.

Electronic supplementary material The online version of this article (https://doi.org/10.1007/s11104-020-04465-9) contains supplementary material, which is available to authorized users.

H. Zou · J. Chen (✉) · G.-H. Wei (✉)
State Key Laboratory of Crop Stress Biology in Arid Areas, College of life sciences, Northwest A&F University, 3 Taicheng Road, Yangling, Shaanxi 712100, People's Republic of China
e-mail: chenjuan@nwsuaf.edu.cn
e-mail: weigehong@nwafu.edu.cn

H. Zou · G.-H. Wei
Shaanxi Key Laboratory of Agricultural and Environmental Microbiology, Yangling, Shaanxi 712100, People's Republic of China

N.-N. Zhang · X.-Y. Lin · W.-Q. Zhang · J. Chen
State Key Laboratory of Soil Erosion and Dryland Farming on the Loess Plateau, Northwest A&F University, Yangling, Shaanxi 712100, People's Republic of China

J.-H. Zhang
School of Life Sciences and State Key Laboratory of Agrobiotechnology, The Chinese University of Hong Kong, Hong Kong, People's Republic of China

J.-H. Zhang
Department of Biology, Hong Kong Baptist University, Hong Kong, People's Republic of China

increased protein carbonyl content and decreased O_2^- scavenging ability was observed in ΔCSE root nodules. Transmission electron microscopy revealed that an H_2S deficit caused the deformation of bacteroids and damage of peribacteroid membranes in nodule cells. Moreover, the expression of some rhizobial and soybean genes related to antioxidant defense was up-regulated in Δ*CSE* nodules.

Conclusion H_2S is crucial for the nitrogen-fixation ability of soybean nodules by acting as an antioxidant element that protects nodule cells and bacteroids from oxidative damage.

Keywords Hydrogen sulfide · Soybean root nodule · Nitrogenase activity · Oxidative stress · Antioxidant defense · Rhizobia

Introduction

For a long time, hydrogen sulfide (H_2S) was considered to be a cytotoxic gas until studies revealed its physiological regulatory effects in animals (Szabó 2007; Yang et al. 2008). More recently, the involvement of H_2S in plant physiological processes has also become a popular area of research (Lisjak et al. 2013; Filipovic and Jovanovic 2017). In plants, H_2S has been proved to participate in root formation and seed germination (Zhang et al. 2008; Zhang et al. 2009). It was reported that H_2S also acts as a regulator of photosynthesis and autophagy in plant cells (Chen et al. 2011; Alvarez et al. 2012; Laureano-Marín et al. 2016). Recently, it has been found that H_2S may change the structures and activities of target proteins via persulfidation of reactive cysteine residues. This occurs via the conversion of the thiol group (-SH) into a persulfide group (-SSH) (Aroca et al. 2017a). Moreover, numerous studies have demonstrated the protective effects of H_2S against oxidative damage in plants caused by abiotic stresses including heavy metal, heat, drought, hypoxia, and salt stress (Wang et al. 2010; Zhang et al. 2008; Li et al. 2012; Cheng et al. 2013; Shi et al. 2013; Chen et al. 2016).

In mammals, endogenous H_2S is mainly produced by two L-cysteine (L-Cys) metabolism-related enzymes, cystathionine γ-lyase (CSE), and cystathionine β-synthase (CBS) (Wang 2002; Qu et al. 2008). In plant cells, it has been reported that L-Cys desulfidrase (LCD) is mainly responsible for H_2S generation (Alvarez et al. 2010). Moreover, another pyridoxal 5′-phosphate (PLP)-dependent enzyme β-cyanoalanine synthase (CAS) is presumed to contribute to H_2S formation by converting cysteine and cyanide to H_2S and β-cyanoalanine (Cheng et al. 2013). Furthermore, in microorganisms, a very early studies demonstrating H_2S production in *Shigella alkalescens* (Galton and Hess 1946). However, recent studies have been reported that bacteria endogenously produce H_2S via 3-mercaptopyruvate sulfurtransferase (3MST) or CSE (Shatalin et al. 2011; Wu et al. 2015). It is worth noting that the production of H_2S in *Escherichia coli* and some other pathogenic bacteria has been reported to be crucial for their survival against antibiotics (Shatalin et al. 2011). Furthermore, a recent study has proved that the 3MST-mediated endogenous production of H_2S may suppress oxidative stress in *E. coli* by sequestering free iron required to drive the genotoxic Fenton reaction (Mironov et al. 2017). So far, various studies have been reported the link between H_2S and the virulence of pathogenic bacteria. Grosshennig et al. (2016) suggested that HapE, a bifunctional enzyme that generates H_2S, could enhance the virulence of *Mycoplasma pneumoniae*, leading to hemolysis in the infected host. Soutourina et al. (2010) reported that the deletion of the regulator of cysteine metabolism (*CymR*) gene, in the human pathogen *Staphylococcus aureus*, promoted H_2S production and enhanced bacterial survival inside macrophages. Furthermore, Peng et al. (2017) also found that H_2S-mediated S-sulfidation may modulate the expression of secreted virulence factors and the cytotoxicity of the secretome in *S. aureus*.

Contrary to the pathogenic infection mechanism, the symbiosis between legume plants and rhizobia leads to the formation of a specialized organ known as the root nodule. After infection, which is strictly regulated by the host plant, rhizobia are released from infection threads into nodule cells where they substantially differentiate into bacteroids. These bacteroids fix atmospheric dinitrogen (N_2) into ammonia for the usage of their plant host. In legume root nodules, high rates of respiration are required due to the high energy consumption of nitrogen (N) fixation (Becana et al. 2001). Nodules are rich in strongly reducing compounds, polyunsaturated fatty acids, and O_2-labile proteins including nitrogenase (Nase) itself. This strongly reducing environment in nodules promotes the generation of reactive oxygen species (ROS) (Dalton 1995; Santos et al. 2000). Early studies have reported that root nodules possess a high capacity for producing ROS (Hunt and Layzell 1993).

Thus, to resist the oxidative damage caused by ROS, antioxidant defenses are necessary to maintain N fixation in root nodules. Our recent study has found that exogenous H_2S treatment could promote nodulation and Nase activity in soybean (*Glycine max*) nodules formed with rhizobia (*Sinorhizobium fredii*) (Zou et al. 2019). However, whether endogenous H_2S is produced in soybean root nodules and involved in the antioxidant system remains unclear.

In the present study, our main objective was to investigate the antioxidant role of H_2S in *G. max-S. fredii* symbiotic root nodules, and the mechanism of how H_2S regulates the N-fixation process in soybean nodules. Genome sequencing was used to find the *CSE* gene and *3MST* genes in the *S. fredii* strain Q8, which could be the main elements responsible for producing endogenous H_2S in soybean nodules. The results demonstrated substantial H_2S production in soybean nodule cells. The presence of H_2S was crucial for maintaining the Nase activity. Soybean nodules with impaired H_2S production exhibited decreased Nase activity, higher H_2O_2 accumulation, higher lipid oxidation, higher protein oxidation, and decreased O_2^- scavenging ability. Moreover, an H_2S deficit in soybean nodules stimulated antioxidant defense responses. Altogether, the present study implied that H_2S has a crucial role in maintaining N fixation in soybean root nodules by functioning as an antioxidant element. This may reveal a new physiological effect of H_2S in the legume-rhizobia symbiotic system and provide a new solution to reducing the overuse of nitrogen fertilizers in soybean production.

Materials and methods

Bacterial culture

For the rhizobial culture, TY medium (5 g/L tryptone, 3 g/L yeast extract, and 0.5 g/L $CaCl_2$) was used. Free-living *S. fredii* was shake-cultured (180 rpm) in liquid TY medium for 72 h at 28 °C and then collected by centrifuging (8000×*g*). For the *E.coli* culture, lysogeny broth medium (10 g/L tryptone, 5 g/L yeast extract, and 10 g/L NaCl) was used.

Plasmid construction

The primers used to construct the *CSE* deletion mutant and the complementation strains are listed in Table S1. Primers *CSE*-U1 and *CSE*-U2 were used to amplify an 800-bp upstream fragment of *CSE* with an EcoRI restriction enzyme site at the 5′ end and a 25-bp homologous sequence of *CSE* downstream at the 3′ end. The primers *CSE*-D1 and *CSE*-D2 were used to amplify the 800-bp downstream fragment of *CSE* containing a 25-bp homologous sequence of *CSE* upstream at the 5′ end and a BamHI site at the 3′ end. The two fragments were then combined using overlap extension PCR with the *CSE*-U1 and *CSE*-D2 primers using standard protocols (Liu and Naismith 2008). The fused fragment was checked and recycled by agarose gel electrophoresis. Then the fused fragment was cloned into the plasmid pk18mobsacB and digested with the EcoRI and BamHI enzymes to generate plasmid pK18CSE, which was verified by sequencing.

To construct the plasmid for *CSE* complementation, we used the primers *CSE*-CP1 and *CSE*-CP2 to amplify a DNA fragment containing a putative promoter of *CSE* (300 bp upstream of *CSE*) and full-length *CSE* with an EcoRI restriction enzyme site at the 5′ end and an XbaI restriction enzyme site at the 3′ end. The PCR product was then purified using a Universal DNA Purification Kit (Tiangen, Beijing, China). The purified PCR product was cloned into the plasmid pBBR1MCS-5 and digested with EcoRI and XbaI to generate the complementation plasmid pBBRCSE, which was verified by sequencing.

Construction of the *S. fredii* ΔCSE and CpΔCSE strains

To construct the deletion mutant Δ*CSE* strain, we first transformed pK18CSE into the *E. coli* strain DH5α to generate DH-CSE. Then a triparental mating procedure was used, as described previously (Saegesser et al. 1992), to transform pK18CSE from DH-CSE into *S. fredii*. Briefly, cultures of *E. coli* DH-CSE (absorbance at 600 nm, $OD_{600} = 0.5$), *E. coli* DH-2013 ($OD_{600} = 0.5$), and *S. fredii* ($OD_{600} = 0.5$) were mixed (v:v:v = 1:1:4) and cultured on a TY agar plate for 7 d. Single exchange (plasmid pK18CSE integrated into genomic DNA of *S. fredii*) cells of *S. fredii* were selected using SM agar plates containing kanamycin (10 g/L mannitol, 0.5 g/L K_2HPO_4, 0.5 g/L KNO_3, 0.2 g/L $MgSO_4 \cdot 7H_2O$, 0.1 g/L $CaCl_2$, 0.1 g/L NaCl, 50 μg/mL kanamycin). The double-exchange mutant (Δ*CSE* strain) was then isolated using TY agar plates containing sucrose (5 g/100 mL). Both single-exchange and double-exchange mutants were verified by colony

PCR and sequencing. For genetic complementation, pBBRCSE was transformed from *E. coli* DH-CPCSE into *S. fredii* by triparental mating. SM agar plates containing gentamicin were used to isolate the complementation mutant (Cp*ΔCSE*), while colony PCR and sequencing were used to verify the mutant strain. All the bacterial strains and plasmids used in this study are listed in Table 1.

Plant growth and treatment

Soybean (*Glycine max* cv. Zhonghuang 13) seeds were surface-sterilized with 75% ethyl alcohol and sodium hypochlorite and then placed on a 1% agar plate for 72 h at 28 °C in the dark. Eight hundred milliliters of growth medium (vermiculite and perlite, v:v = 1:1) was watered with 400 mL of N-free nutrient solution (100 mg/L $CaCl_2$, 100 mg/L KH_2PO_4, 5 mg/L ferric citrate, 150 mg/L NaH_2PO_4, 240 mg/L $MgSO_4$, 2.86 mg/L H_3BO_3, 2.03 mg/L $MnSO_4{\cdot}4H_2O$, 0.22 mg/L $ZnSO_4{\cdot}7H_2O$, 0.06 mg/L $Na_2MoO_4{\cdot}2H_2O$, and 0.08 mg/L $CuSO_4{\cdot}5H_2O$) and sterilized in a polypropylene planting bag. Germinated seeds were transferred into the growth medium (one seedling per bag). Ten days after transferring the seedling into the medium, each seedling was inoculated with a 10-mL suspension of the WT, Δ*CSE*, or Cp*ΔCSE S. fredii* strain. Nodules were harvested at 7, 14, and 28 DPI. Plants were grown in a controlled growth chamber with a light/dark regime of 16/8 h, relative humidity of 80%, a temperature of 27 °C, and photosynthetically active radiation of 280 μmol/m^2/s.

To artificially change the H_2S content in soybean root nodules, we used NaHS and hypotaurine (HT) to pretreat soybean root nodules. The freshly harvested root nodules were prepared by soaking them in 100 μM NaHS or 0.3 mM HT solutions for 1 h at 28 °C, and washing them with 100 mM phosphate-buffered saline.

Visualization of H_2S and H_2O_2 with fluorescent probes

The H_2S fluorescent probe SF7-AM and the H_2O_2 fluorescent probe PO-1 were purchased from Sigma-Aldrich (CAS: 1416872–50-8 and 1,199,576–10-7; Dallas, USA). Fresh nodule slices (80 μm thick) were obtained with a freezing microtome (Tissue-Tek, Sakura, Japan). As described by Lin et al. (2013), nodule slices were washed with phosphate buffer (pH = 7.4), incubated in 5 mM SF7-AM or PO-1 for 1 h, and washed with 20 mM HEPES. The samples were visualized and photographed using an Andor Revolution confocal microscope (Andor Technology, Belfast, Northern Ireland). An excitation wavelength (λex) of 488 nm was used to detect the green fluorescent signal of SF7-AM, and a λex of 561 nm was used for the detection of the PO-1 signal. The merging of fluorescent pictures and

Table 1 Bacterial strains and plasmids used in this study. Km^r, Kanamycin resistance; Gm^r, Gentamicin resistance

Strain or plasmid	Description	Source
Escherichia coli		
DH5α	*endA hsdR17 supE44 thi-1 recA1 gyrA relA1* Δ(*lacZYA-argF*)*U169 deoR* [*Φ80 dlac*Δ(*lacZ*)*M15*]	Hanahan (1983)
DH-2013	DH5α carries pRK2013 plasmid; Km^r	Afendra and Drainas (1987)
DH-CSE	DH5α carries pK18CSE plasmid; Km^r	This study
DH-CP	DH5α carries pBBRCSE plasmid; Gm^r	This study
Sinorhizobium fredii		
WT	Wild-type	This study
Δ*CSE*	*S. fredii* CSE null mutant	This study
Cp*ΔCSE*	Δ*CSE* carries pBBRCSE plasmid; Gm^r	This study
Plasmids		
pRK2013	Conjugation helper plasmid; Km^r	Afendra and Drainas (1987)
pK18mobsacB	Suicide vector derived from plasmid pK18; Mob^+ *sacB* Km^r	Harrison et al. (2012)
pBBR1MCS-5	Broad-host-range clone vector; Gm^r	Kovach et al. (1995)
pK18CSE	pK18mobsacB::*CSE*	This study
pBBRCSE	pBBR1MCS-5::*CSE* promoter::*CSE*	This study

respective bright-field pictures was conducted with ImageJ (National Institutes of Health, Bethesda, USA).

H_2S determination

The endogenous H_2S content in soybean nodules was assayed using the methylene blue method described by Zhang et al. (2008). The calibration curve was made with NaHS solution concentrations. The H_2S content was measured at OD_{667} with an EPOCH ultraviolet spectrophotometer (BioTek Instruments, Vermont, USA).

The quantification of H_2S in liquid TY media was conducted as reported by Wu et al. (2015). Properly diluted aliquots (1.6 mL) were mixed with 0.2 mL of N, N-dimethyl-p-phenylenediamine sulfate (20 mM in 7.2 M HCl) and 0.2 mL of $FeCl_3$ (30 mM in 1.2 M HCl). After 30 min of reaction at 25 °C, the absorbance at 667 nm was measured and related to sulfide concentration using calibration curves generated with NaHS.

The production of H_2S by free-living *S. fredii* was monitored using a lead acetate detection method (Shatalin et al. 2011). Paper strips saturated with 2% of $Pb(Ac)_2$ were fixed to the inner wall of a culture tube, above the level of the liquid culture. Overnight cultures of *S. fredii* strains were used to inoculate fresh TY medium to $OD_{600} = 0.01$. After incubation (24 h, 28 °C), the paper strips were collected and photographed.

Nase activity assay

Nase activity was assayed using the acetylene reduction assay (ARA) method as described by Fishbeck et al. (1973) with slight modifications. Fresh soybean root nodules were transferred into a 10-mL rubber-capped airtight glass bottle filled with a mixture of acetylene and air (v:v = 1:100). Bottles were incubated at 28 °C for 3 h and the concentration of ethylene was determined using a gas chromatography system (Agilent Technologies, La Jolla, USA).

Biomass accumulation and N content determination

Plant samples at 28 DPI were harvested and dried at 65 °C for 72 h to constant weight. Dry matters were then weighed to determine biomass accumulation.

After the biomass determination, dried plant samples were used for total N content determination. We used the Kjeldahl method reported by Zdravko et al. (2014) with slight modifications. 0.3 g dried plant samples were grounded with mortar and pestle. 5 ml 98% H_2SO_4 was added and mixed with the sample powder. Then the mixture was digested at 365 °C for 2 h. During the digestion, 1.5 mL of H_2O_2 was added into the system every 30 min. Finally, the digestion solution was diluted to a constant volume with distilled water, and the N content was determined using an automatic Kjeldahl apparatus (Kjeltec™ 8400, FOSS, Denmark).

Transmission electron microscopy

Soybean root nodules at 28 DPI were observed using a TECNAI G2 SPIRIT BIO transmission electron microscope (FEI, Oregon, USA) to detect the micromorphological differences between Δ*CSE* and WT nodules. Sample preparation was carried out as described by Yuan et al. (2017) with slight modifications. Soybean nodules were gently washed and the clean root nodules were cut into slices approximately 0.5 mm thick, pre-fixed in 4% glutaraldehyde for 24 h, washed with 0.1 M phosphate-buffered saline (pH = 6.8), and post-fixed in 1.0% osmium tetroxide for at least 3 h. Thereafter, nodules were dehydrated in an ascending ethanol series and embedded in LR white resin. Thin sections were excised from the embedded samples using an EM-UC7 ultramicrotome (Leica, Nussloch, Germany) equipped with a glass knife. Ultrathin sections were mounted on copper grids for TEM examination.

Isolation of bacteroids

The isolation of bacteroids from soybean root nodules was conducted with the method described by Reibach et al. (1981) with slight modification. The nodules were removed from the roots and washed. 5 g of nodules were gently crushed with a mortar and pestle on ice in grinding buffer (0.15 M NaCl and 50 mM KH_2PO_4, pH 7.6). The crude homogenate was filtered through filter paper. The filtrate was collected in centrifuge tube for further use. The residue was then washed with 10 mL of grinding buffer. Add 30 mL of 70% percoll concentrate ($\rho = 1.09$ g/cm^3) containing 24.5 mL percoll concentrate, 3.5 mL of 0.5 M KH_2PO_4 and 1.5 M NaCl, and 7 mL of ddH_2O into 50 mL centrifuge tube.

Add 1 g of the filtered crude extract onto the top of percoll concentrate. The tube was then centrifuged for 2 h at 15000×g. Bacteroids were transferred to a new centrifuge tube. Percoll was removed by diluting the bacteroid fraction (underlying substance) 1:5 with 0.15 M NaCl plus 50 mM KH_2PO_4, pH 7.6, and centrifuging at 12000×g for 10 min. The bacteroid pellet was then resuspended in 0.15 M NaCl plus 50 mM KH_2PO_4, pH 7.6. The rest part were then mixed with filtrate previously acquired and used as nodule homogenate for experiment.

Determination of oxidative damage

To determine H_2O_2 content in soybean root nodules, we used the method described by Liu and Naismith (2008). Briefly, H_2O_2 was extracted from 0.5 g of freshly harvested soybean root nodules in 2 mL of cold acetone with a mortar and pestle. The homogenate was centrifuged at 6000×*g* for 25 min. Subsequently, 1 mL of extracted solution was mixed with 0.2 mL of 20% titanium sulfate in concentrated HCl. This was followed by the addition of 0.4 mL of 25% aqueous solution of ammonia to precipitate the peroxide-titanium complex. The mixture was then centrifuged at 6000×*g* for 15 min. The precipitate was solubilized in 1 mL of 2 M H_2SO_4 and brought to a final volume of 2 mL. The absorbance of the obtained solution was read at 415 nm against water blank. A standard response curve was prepared with known concentrations of H_2O_2 using the same method as described above.

For the MDA content measurement, we referred to the protocol of Redondo et al. (2009) with slight modification. 0.5 g sample was homogenized with 2.5 mL of 0.1% trichloroacetic acid (TCA) using a mortar and pestle on ice. The homogenate was centrifuged for 10 min at 12000×g. Then, 2 mL of supernatant was added to 2 mL of 0.67% thiobarbituric acid in TCA. The mixture was boiled for 20 min and then cooled at room temperature. The mixture was then centrifuged for 15 min at 12000×g and the absorbance of the supernatant was measured at 450, 532 and 600 nm. The MDA content (μmol/g FW) was calculated using the following formula.

$$C_{MDA}\ (\mu mol/L) = 6.45 \times (OD_{532} - OD_{600}) - 0.56 \times OD_{450}.$$

$$\text{MDA content} = (C_{MDA} \times V)/(Vs \times m \times 1000).$$

C_{MDA} : MDA concentration in reaction mixture (μmol/L).V : Total volume of sample extracts (mL).Vs : Volume of sample extract used for measurement.

For measuring the protein carbonyl content in soybean root nodules, we used a Comin protein carbonyl assay kit (Comin Biotechnology, Suzhou, China) following the manufacturer's instructions. Protein carbonyl content was measured using OD_{370}. The O_2^- radical scavenging ability was assayed using a superoxide anion scavenging ability assay kit (Comin Biotechnology Co., Ltd., Suzhou, China). All the procedures were conducted following the manufacturer's instructions. O_2^- scavenging ability was calculated using OD_{530}.

Enzymatic activity assay

The activities of SOD, CAT, and TrxR were measured using enzymatic activity assay kits purchased from Comin biotechnology (Suzhou). The whole procedure was conducted following the instructions from the manufacturer. SOD, CAT, and TrxR activities were measured at OD_{560}, OD_{240}, and OD_{412}, respectively with an EPOCH ultraviolet spectrophotometer (BioTek, Vermont, U.S.A).

GSH, nicotinamide adenine dinucleotide phosphate (NADP[H]) and total thiols quantification.

GSH content in nodule tissues was determined with the method described by (Matamoros et al. 1999) with slight modification. 0.1 g of nodule tissue was added to 1 mL of 0.1 M HCl. The mixture was then shaken at room temperature for 1 h. After centrifugation at 15000 g for 20 min, 100 μL of the supernatant was added into 100 μL of 2-(cyclohexylamine)ethane sulphonic acid (CHES), adjust to pH 8.5. Then add 70 μL of 100 mM DTT into the system. The mixture was then incubated at 28 °C for 1 h. Add 10 μL of 18 mM monobromobimane (mBBr) and incubated in dark for 30 min. After the incubation, 200 μL of 10 mM methyl sulphonic acid was added into the mixture. The samples were centrifuged at 20000 g for 40 min and then filtered through a 0.2 lm nylon filter, and separation of thiols was conducted on an Agilent Hypersil BDS-C18 column using an HP1100 HPLC system. Mixed standards treated exactly as the sample supernatants were used as a reference for the quantification of cysteine and GSH content.

For NADP(H) determination, pyridine nucleotides were extracted from 30 mg of nodules with 23 0.5 mL of 0.1 m NaOH (NADH and NADPH) or with 2 × 0.5 mL of 5% (*w*/*v*) TCA (NAD1 and NADP1) at room temperature. After thorough homogenization for 90 to 120 s in an Eppendorf tube, the extracts were boiled for 6 min, cooled on ice, and centrifuged at 13,000 g for 6 min at room temperature. The supernatant (25 mL) was made up to 100 mL with NaOH or TCA, and the nucleotides were quantified by the enzymatic cycling method of Matsumura and Miyachi (1980).

The amounts of total thiols were measured using the method described by Aravind and Prasad (2005). 0.5 g of nodule tissue was added into 0.02 M EDTA and homogenized with pestle and mortar. The mixture was centrifuged at 15,000 g for 10 min. Reaction mixture containing 50 mL sample, 150 ml 0.2 M Tris/HCl pH 8.2, 10 mL DTNB and 790 mL methanol was incubated for 15 min at room temperature. The absorbance was determined at 412 nm.

RNA isolation, reverse transcription and gene expression analysis

Total RNA isolation was performed using the MiniBEST Plant RNA Extraction Kit (Takara, Dalian, China) according to the manufacturer's instructions. After the extraction procedure, we used recombined DNase to erase the genomic DNA. The RNA integrity was examined using 1% agarose gel electrophoresis. The RNA concentration was determined using an EPOCH Microplate Spectrophotometer (BioTek). Reverse transcription was conducted using the PrimerScript™ RT Master Mix (Takara) as suggested by the manufacturer. The qRT–PCR was carried out using a Quantstudio 6 Flex real-time PCR system (Thermo Fisher, Carlsbad, USA) and SYBR Premix Ex Taq II (Takara). The qRT–PCR program is described in Table S3. The primers used for the expression assay were designed with Primer Premier 5.0 (Premier Biosoft International, Palo Alto, USA) according to the coding sequence of the respective gene. The coding sequences were obtained from GenBank (https://cipotato.org/genebankcip/) or the European Molecular Biology Laboratory (https://www.embl.org/). The target fragments amplified by the primers were sequenced and checked by 1% agarose gel electrophoresis to ensure the accuracy of the qRT–PCR reaction. The sequences of the primers used in the present study are listed in Table S2. The qRT–PCR reaction was conducted with three biological replicates and three technical replicates. For the *G. max* gene expression assay, *GmActin* was selected as the endogenous control. For the *S. fredii* gene expression assay, the *16S* ribosomal gene was selected as the endogenous control.

Statistical analysis

Statistical significance of differences between means was tested by the one-way analysis of variance (ANOVA) using SPSS 19.0 (IBM SPSS, Somers, USA). The results are expressed as the mean values ± standard error of at least three independent experiments. Three sets of soybean plants were grown at different times as biological replicates. For the Nase and antioxidant enzymatic activity assays, three biological replicates and five technical replicates were used. For the qRT–PCR assay, three biological replicates and three technical replicates were set. For the TEM and confocal microscopy, at least twenty nodules from different biological replicates were observed. For the H_2S, H_2O_2, MDA, and protein carbonyl determination and the O_2^- scavenging ability assay, three biological replicates and five technical replicates were conducted.

Results

H_2S is generated in soybean root nodules

To detect the presence of H_2S in soybean root nodules, we used the fluorescent probe SF7-AM. Due to the large size of the soybean nodule, it was difficult for the fluorescent probe to completely penetrate into the central zone. Thus, the observation of H_2S fluorescence was conducted using fresh nodule slices (80 μm thick). After loading the SF7-AM probe, a strong green fluorescent signal suggested that H_2S was produced on mass in both young soybean nodules (14 days post-inoculation [DPI]) and mature nodules (28 DPI). This endogenous H_2S production was located in the central N-fixing zone. However, in the nascent soybean nodules (7 DPI), no significant fluorescence was observed (Fig. 1a).

To test the specificity of the fluorescent probe, we used the H_2S scavenger hypotaurine (HT) to treat the

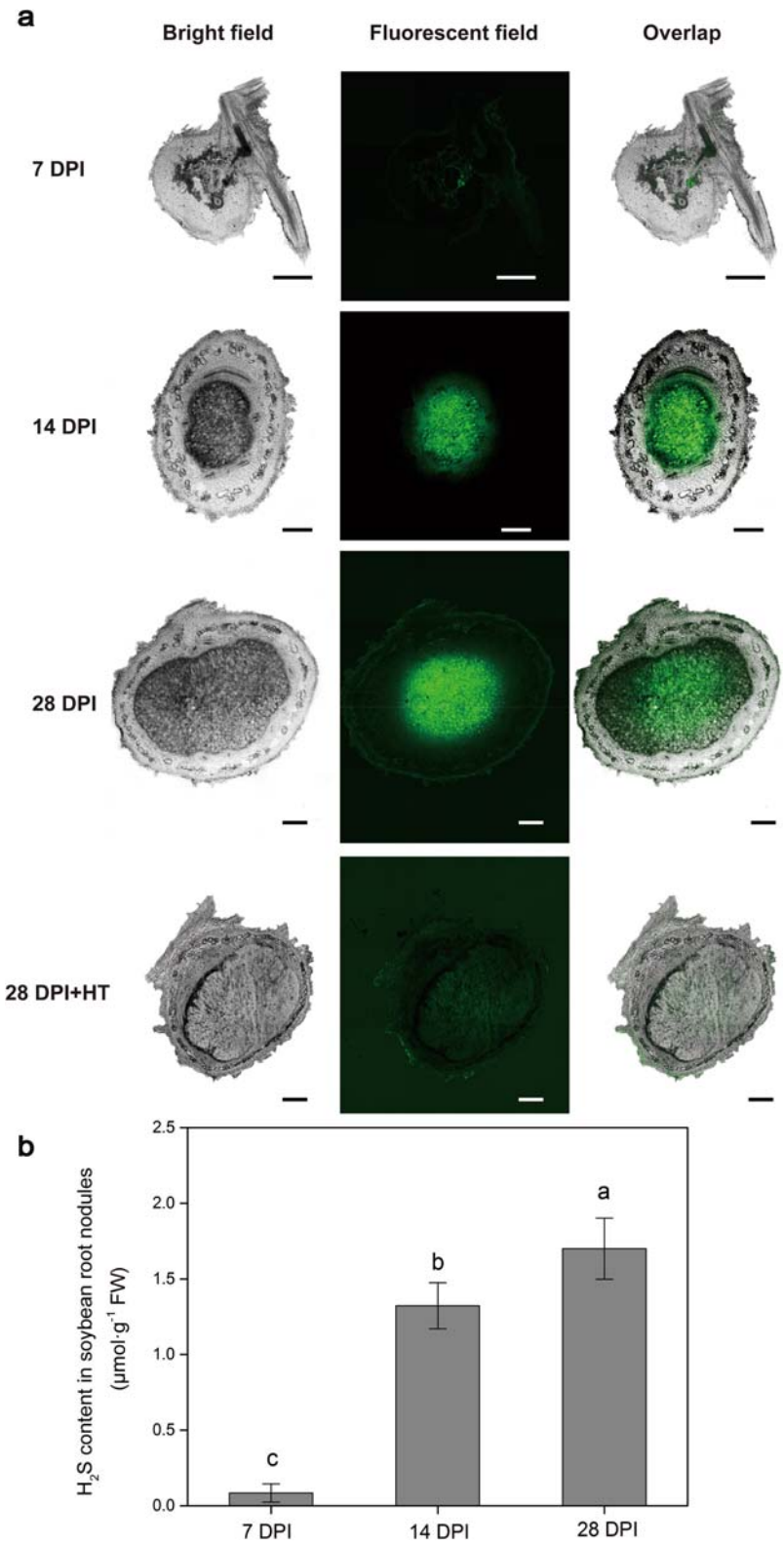

Fig. 1 H_2S production in soybean root nodules. (**a**) Confocal microscopy using the fluorescent probe SF7-AM. Bars = 250 μm. For fluorescent signal detection, excitation wavelength λ_{ex} = 488 nm. HT represents the H_2S scavenger hypotaurine. (**b**) H_2S content at 7, 14, and 28 days post-inoculation (DPI). Error bars represent standard error (SE). Values stand for means ± SE of three independent biological replicates, n = 15. Different letters above the column indicate significant difference between means ($P < 0.05$)

nodule slices before loading the SF7-AM probe. The fluorescent signal was no longer present in the 28-DPI nodule slices pretreated with 0.3 mM HT (Fig. 1a). We then determined the H_2S content in soybean root nodules using the methylene blue method. The H_2S content reached 1.734 μmol/g fresh weights (FW) at 28 DPI, which was higher than at 7 DPI (0.085 μmol/g FW) and 14 DPI (1.323 μmol/g FW; Fig. 1b). These results were consistent with the SF7-AM assay (Fig. 1a).

Deletion of the CSE gene in *S. fredii* impairs H_2S production

The variation in H_2S production from soybean root nodules at different stages suggests that H_2S may be related to the N-fixation ability of the nodules. To further test the correlation between H_2S production and N fixation in soybean nodules, we constructed a *S. fredii* mutant strain by deleting the *CSE* gene. The staining test with a 2% lead acetate test paper showed that H_2S production in the Δ*CSE* mutant (indicated by brown color) was strongly inhibited under free-living conditions (Fig. 2a). We then combined the coding sequence of the *CSE* gene under the regulation of its native promoter into the plasmid pBBR1MCS-5 to construct the complementary strain (CpΔ*CSE*). The complementation of the *CSE* gene successfully rescued the impaired H_2S production capacity. The total H_2S production in the Δ*CSE* mutant decreased to ~25% of that of the wild-type (WT) *S. fredii* in liquid tryptone-yeast (TY) medium under free-living conditions. H_2S production was fully restored in CpΔ*CSE* nodules (Fig. 2a).

Under symbiotic conditions, the Δ*CSE* strain successfully established a symbiosis with soybean plants and formed root nodules (Δ*CSE* nodules) with a normal appearance similar to WT nodules. Quantification of H_2S found that the H_2S content in Δ*CSE* nodules was 1.237 μmol/g FW, only half of that found in WT nodules. The complementation of *CSE* rescued the H_2S production capacity in CpΔ*CSE* nodules (Fig. 2b). The SF7-AM assay also showed that H_2S content in Δ*CSE* nodules was significantly lower than in WT nodules, whereas no significant difference was observed for the H_2S content between CpΔ*CSE* nodules and WT nodules (Fig. 2c).

Taken together, these results suggest that the deletion of the *CSE* gene in *S. fredii* strongly inhibited H_2S production in soybean nodules.

Deletion of the CSE gene in *S. fredii* leads to loss of Nase activity

To investigate the possible correlation between H_2S content and N-fixation ability, we determined Nase activity in soybean nodules. At 28 DPI, which is usually the peak of the N-fixation ability of soybean root nodules, the Nase activity in Δ*CSE* nodules was significantly lower than in WT nodules; however, comparable Nase activity was found in CpΔ*CSE* and WT nodules (Fig. 3a). To ensure that this variation in Nase activity was due to the change in H_2S content, we used sodium hydrosulfide (NaHS) as an exogenous H_2S donor to pretreat the Δ*CSE* nodules. After the 100 μM NaHS pretreatment, the Nase activity in Δ*CSE* nodules partially recovered. We also used the H_2S scavenger HT to pretreat the soybean root nodules. WT nodules treated with 0.3 mM HT exhibited a 27.1% loss of Nase activity compared with the non-treated WT nodules (Fig. 3a).

Quantification of H_2S in soybean nodules confirmed that the 100 μM NaHS pretreatment significantly increased the H_2S content in soybean nodules compared with the non-treated Δ*CSE* nodules. The HT treatment also caused a decrease in the H_2S content of WT nodules (Fig. 3b). In general, the Nase activity correlated with the H_2S content in soybean root nodules. Besides, biomass and N content determination provide further evidence that diminished H_2S level could impact the N assimilation of soybean plants. We observed that the inoculation of WT, Δ*CSE* and CpΔ*CSE* strains showed no significant effect on the biomass accumulation in soybean plants (Fig. 4a and b). However, total N content in soybean plants inoculated with Δ*CSE* strain was lower than that in WT inoculated soybean plants. Moreover, the inoculation of the CpΔ*CSE* strain partially rescued the decrease of N content in soybean roots (Fig. 4c and d).

Taken together, these results highlight that H_2S generation is important to maintain the Nase activity in soybean root nodules.

H_2S may act as part of the antioxidant system in soybean nodules

As Nase activity was strongly inhibited in Δ*CSE* nodules, we investigated the nodulation of soybean plants inoculated Δ*CSE S. fredii* strains. Surprisingly, the deletion of CSE in *S. fredii* Q8 strain displayed no effect on its symbiotic capacity with soybean plants. The results noted that the soybean plants inoculated with WT and

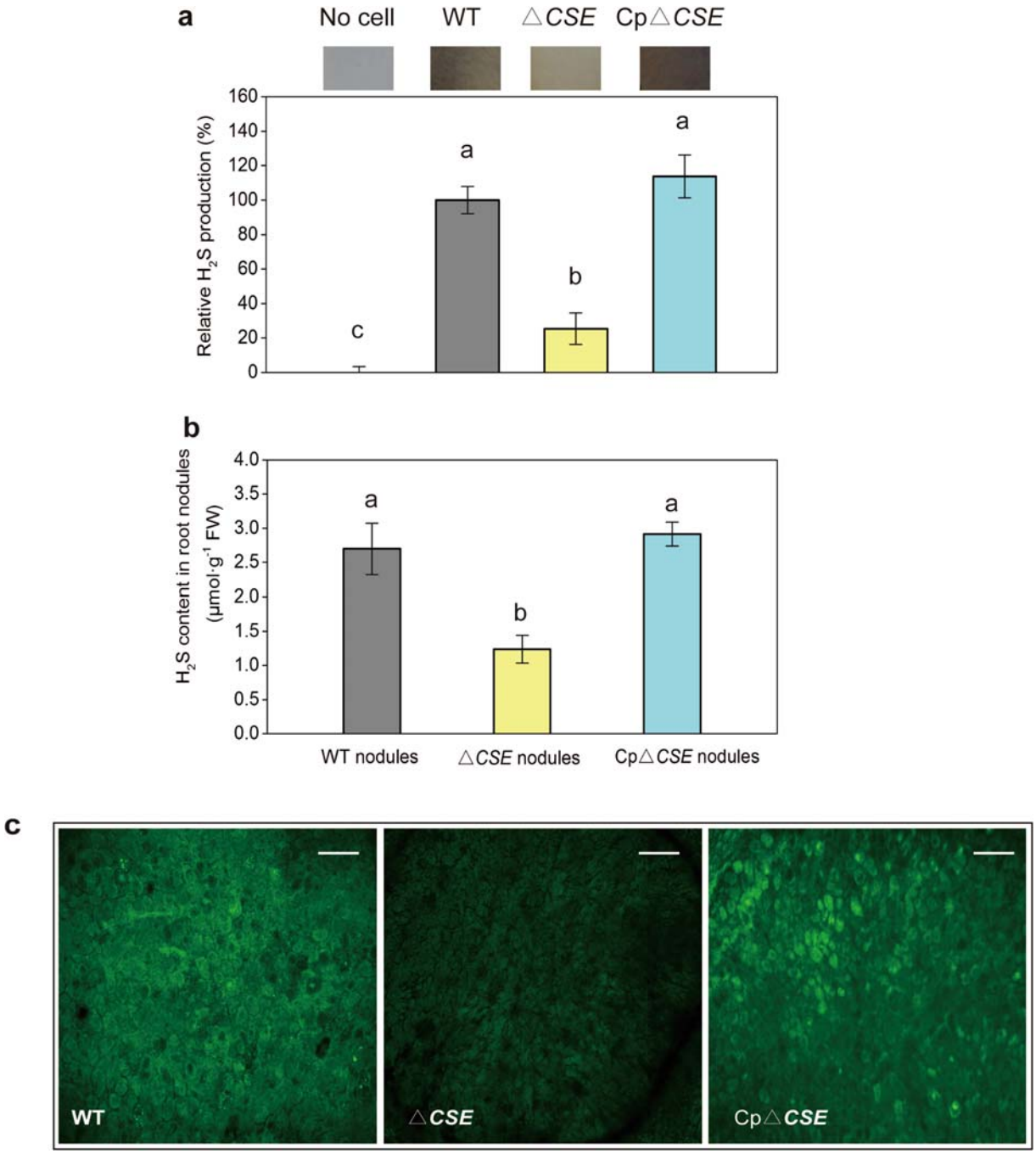

Fig. 2 The H_2S production capacity of free-living *Sinorhizobium fredii* and soybean root nodules. (**a**) H_2S concentration in liquid tryptone–yeast culture of free-living *S. fredii*. Error bars represent standard error (SE), Values stand for means ± SE of three independent experiments, $n = 15$. Different letters above the columns indicate significant differences ($P < 0.05$). For fluorescence detection, excitation wavelength $\lambda_{ex} = 488$ nm. (**b**) H_2S content in soybean root nodules formed with wild-type (WT), *CSE* knock-out mutant (Δ*CSE*), and *CSE* complementary (CpΔ*CSE*) *S. fredii* strains. (**c**) Confocal microscopy of H_2S production using SF7-AM probe in WT, Δ*CSE*, and CpΔ*CSE* nodules. Bars = 100 μm

Δ*CSE* generate about the same number of root nodules (Fig. 5a). Moreover, the Δ*CSE* nodules also failed to exhibit any distinctive morphological features such as size, color, and shape (Fig. 5b, c).

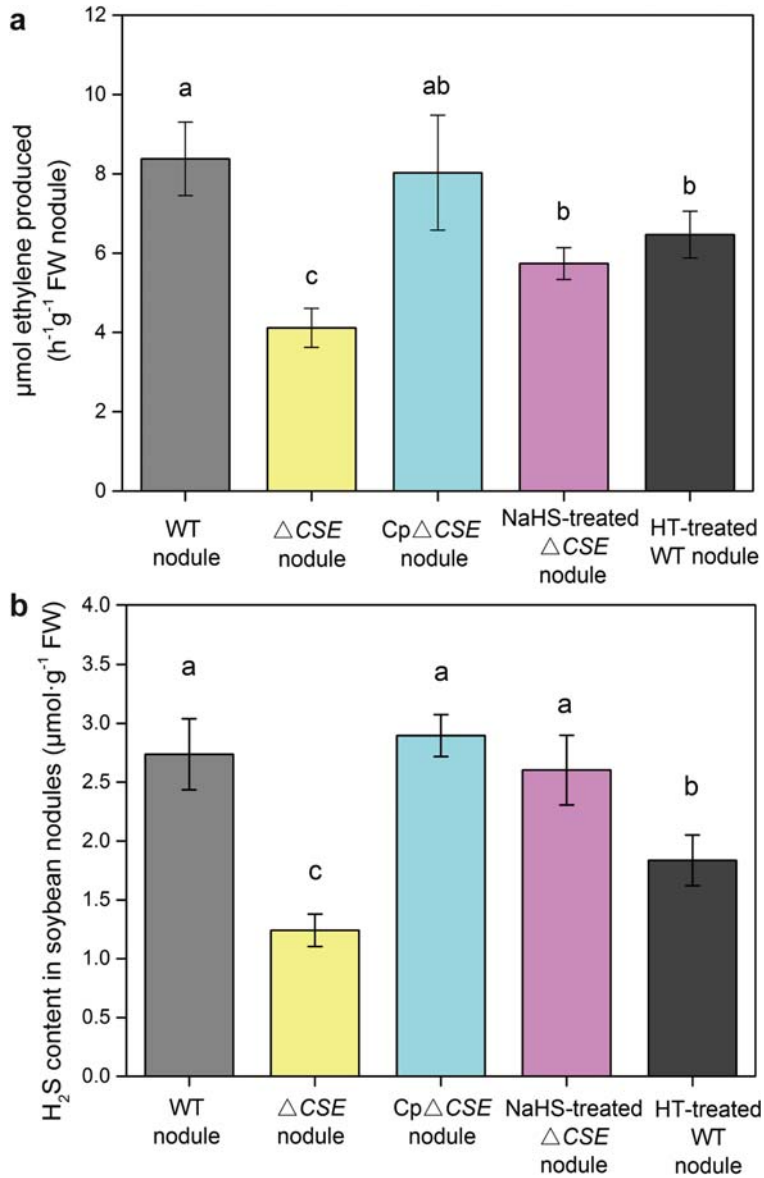

Fig. 3 The nitrogenase activity (**a**) and H_2S content (**b**) in WT, Δ*CSE*, and CpΔ*CSE* nodules. Error bars represent standard error (SE). Values stand for means ± SE of three independent experiments, $n = 15$. Different letters above columns indicate significant differences ($P < 0.05$)

We then conducted transmission electron microscopy (TEM) to determine whether there were structural changes in the nodule cells. Interestingly, in the infected cells, a number of Δ*CSE* bacteroids exhibited deformed traits (Fig. 5e). Compared with WT bacteroids (Fig. 5d), the deformed bacteroids (DFB) exhibited less accumulation of polyhydroxybutyrate (PHB; indicated by bright arrow) and broken peribacteroid membranes (BPM; indicated by a dark triangle).

All these structural characteristics were similar to those previously observed in nodules disordered by ROS, such as senescent nodules and nodules under abiotic stresses (Balestrasse et al. 2004; Li et al. 2008). To clarify whether H_2S could suppress the generation of ROS, we first used fluorescent probes SF7-AM and peroxy orange 1 (PO-1) to observe the presence of H_2S and H_2O_2 in soybean root nodules. PO-1 is a fluorescent probe specific for H_2O_2 detection which can generate a strong orange fluorescent signal in Δ*CSE* nodules after reacting with H_2O_2 (Dickinson et al. 2010). Here, in the present study, we found that the orange fluorescent signal was significantly weaker in WT and CpΔ*CSE* nodules where substantial H_2S was found. The H_2O_2 signal was only observed in the intercellular space of WT and

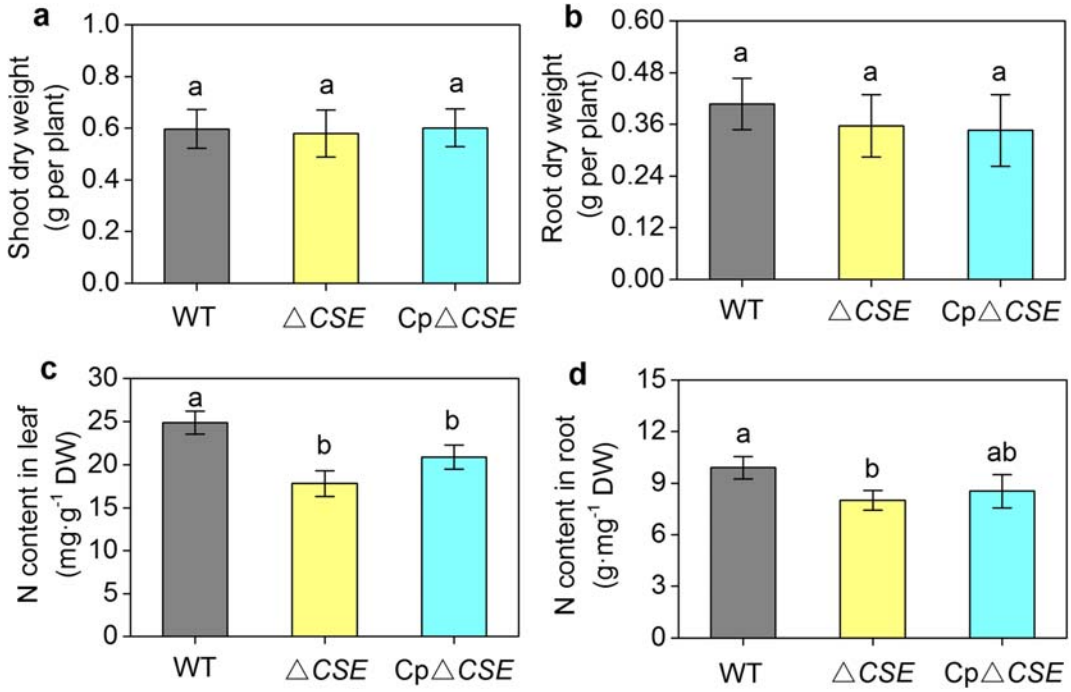

Fig. 4 Soybean plant growth parameters and N content determination. Dry weight of shoots (**a**). Dry weight of roots (**b**). N content in leaves (**c**) and N content in roots (**d**). Error bars represent standard error (SE). Values stand for means ± SE of three independent experiments, $n = 60$. Different letters above columns indicate significant differences ($P < 0.05$)

Cp△*CSE* nodules, whereas H_2O_2 was mainly found in the infected cells of △*CSE* nodules (Fig. 6).

The above results were testified by quantification of H_2O_2 in soybean nodules. The results investigated that at 28 DPI, the H_2O_2 content in △*CSE* nodules was significantly higher than in WT and Cp△*CSE* nodules (Fig. 7a), implying that H_2S content may potentially affect the ROS production in soybean root nodules. To obtain further proof for the potential antioxidant role that H_2S may play in the root nodules, we investigated the oxidative stress-related phenotypes in soybean root nodules. We first measured the total content of carbonyl in the nodule proteins. The carbonyl content was significantly higher in △*CSE* nodules than in WT and Cp△*CSE* nodules (Fig. 7b). We then determined malonaldehyde (MDA) content as a key indicator of lipid peroxidation in root nodules. The MDA content in △*CSE* nodules was significantly higher than in WT and Cp△*CSE* nodules (Fig. 7c), signifying that deficit of H_2S may lead to higher lipid peroxidation in root nodules. To further distinguish whether the oxidative damage mainly occurred in bacteroids or plant cells, we also conducted protein carbonyl and MDA content determination with isolated bacteroids and nodule homogenate without bacteroids. As shown in Fig. S1, MDA content and protein carbonyl contents in both bacteroids and bacteroid-free nodule homogenate are elevated in △*CSE* nodules. This result indicated that deficit H_2S could cause oxidative damage in both rhizobia and plant cells in soybean nodule.. In addition, we compared the O_2^- scavenging ability of the crude extracts from WT and △*CSE* nodules. With a higher H_2S content, the WT nodules possessed a greater O_2^- scavenging ability than △*CSE* nodules (Fig. 7d).

Impaired H_2S generation up-regulates expression of antioxidant genes in *S. fredii* and soybean hosts

To further describe the consequences of impaired H_2S generation in nodules, we investigated the expression levels of antioxidant genes in both bacteroids and plant sections from nodule cells by quantitative reverse transcription-polymerase chain reaction (qRT-PCR). On the rhizobial side, the expression levels of *katE* and *katG*, encoded for CAT, were significantly up-regulated in △*CSE* nodules at 28 DPI (Fig. 8a and b). Moreover, *sodA* and *sodC,* encoded for SOD, also exhibited high expression levels in △*CSE* nodules (Fig. 8c and d).

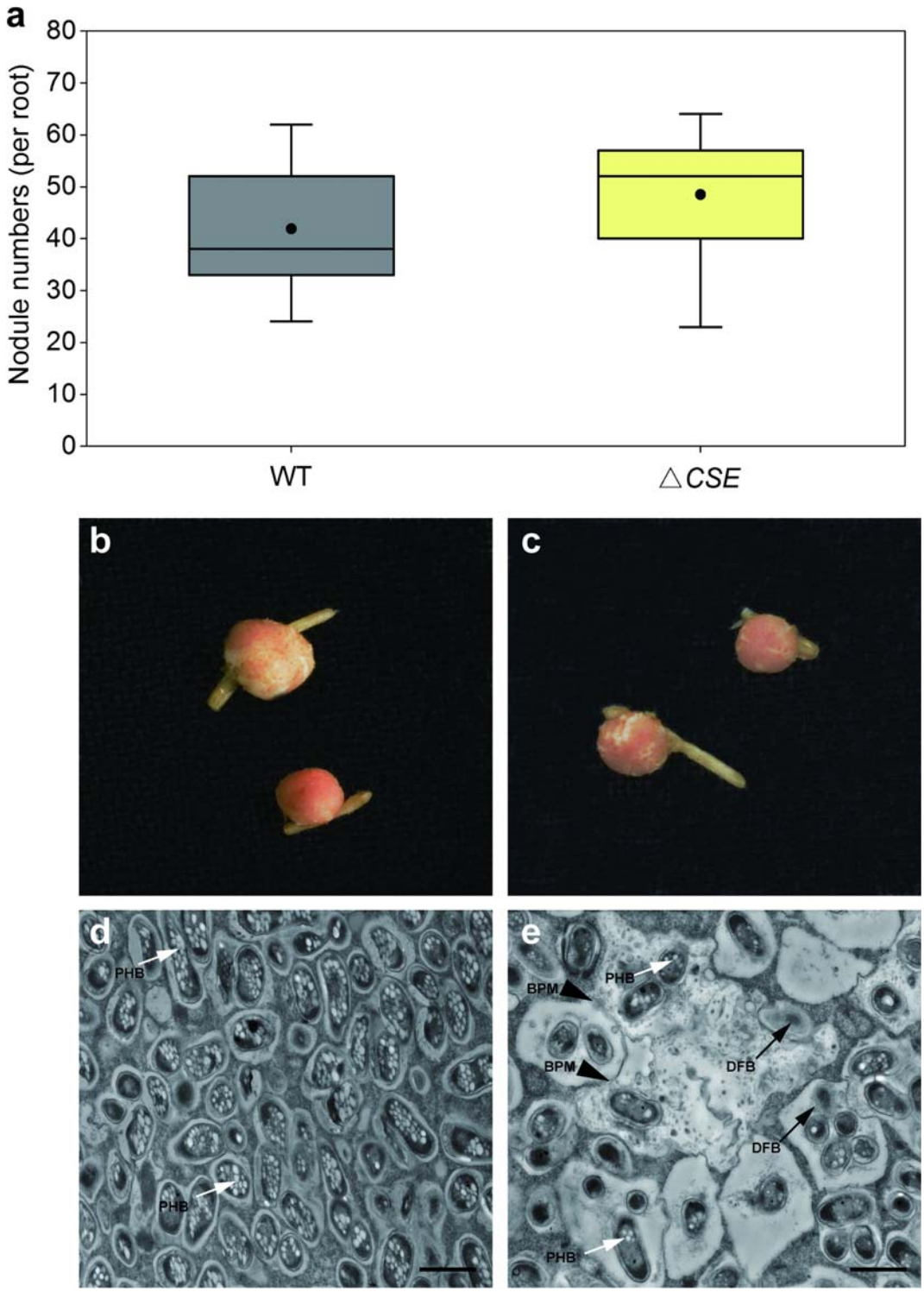

Fig. 5 Nodulation investigation of soybean plants and transmission electron microscopy (TEM) of WT and Δ*CSE* nodule cells at 28 DPI. (**a**) indicates nodule numbers of soybean plants inoculated with WT and Δ*CSE* rhizobia strains at 28 DPI. (**b**) and (**c**) are the photographs taken from WT and Δ*CSE* nodules, respectively. (**d**) and (**e**) are the TEM images taken from WT and Δ*CSE* nodule cells, respectively. Bars = 2 μm. PHB: polyhydroxbutyrate. DFB: deformed bacteroids. BPM: broken peribacteroid membrane. The analysis was conducted with at least 20 nodules as biological replicates. Representative pictures are shown

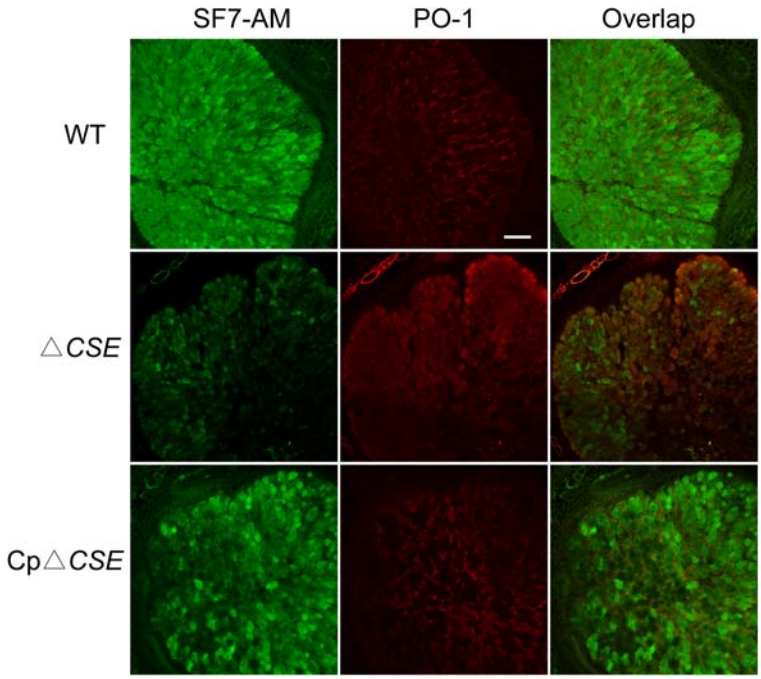

Fig. 6 Confocal microscopy of H_2S (SF7-AM) and H_2O_2 (PO-1) production in WT, Δ*CSE*, and CpΔ*CSE* nodules. For H_2S detection, excitation wavelength λex = 488 nm. For H_2O_2 detection, λex = 561 nm. Bar = 250 μm. The analysis was conducted using at least 20 nodules as biological replicates. Representative pictures are shown

On the plant side, the impaired generation of H_2S led to the up-regulation of several genes that were reported to be involved in the antioxidant defense system. In Δ*CSE* nodules, *GmSOD1* and *GmSODB2,* which encode Cu-Zn SOD and Fe SOD, exhibited higher expression levels than in WT nodules (Fig. 9a and b). The expression level of *GmCAT*, which encodes catalase, was also up-regulated in Δ*CSE* nodules (Fig. 9c).

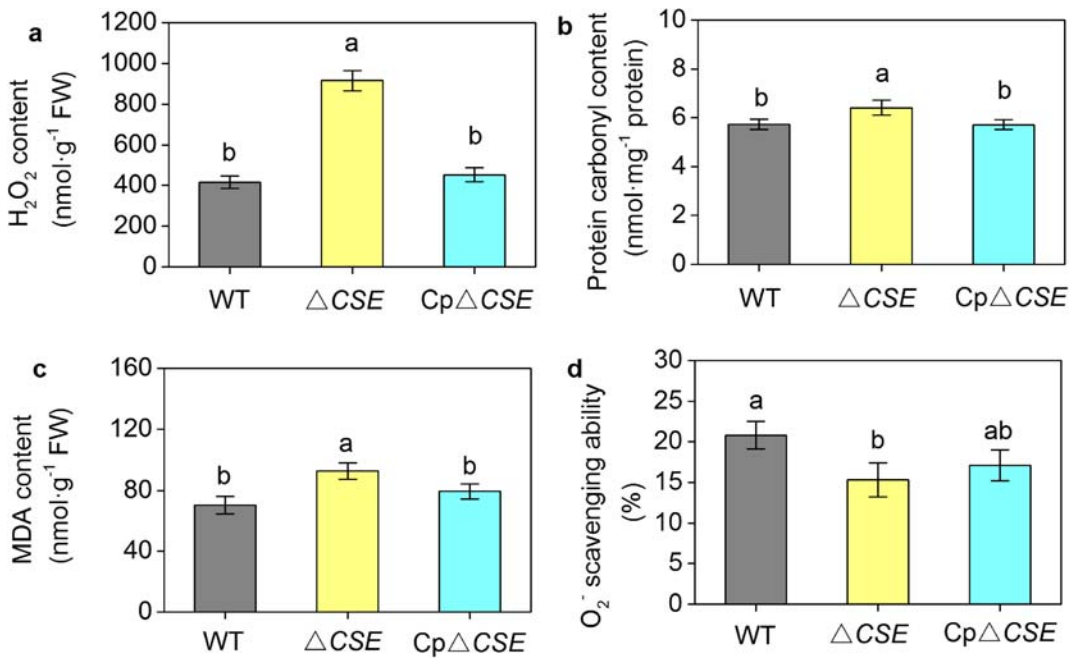

Fig. 7 Oxidative-related parameters in WT, Δ*CSE*, and CpΔ*CSE* nodules. (**a**) H_2O_2 content; (**b**) Protein carbonyl content; (**c**) Malonaldehyde (MDA) content and (**d**) O_2^- scavenging ability. Error bars represent standard error (SE). Values stand for means ± SE of three independent experiments, $n = 15$. Different letters above columns indicate significant differences ($P < 0.05$)

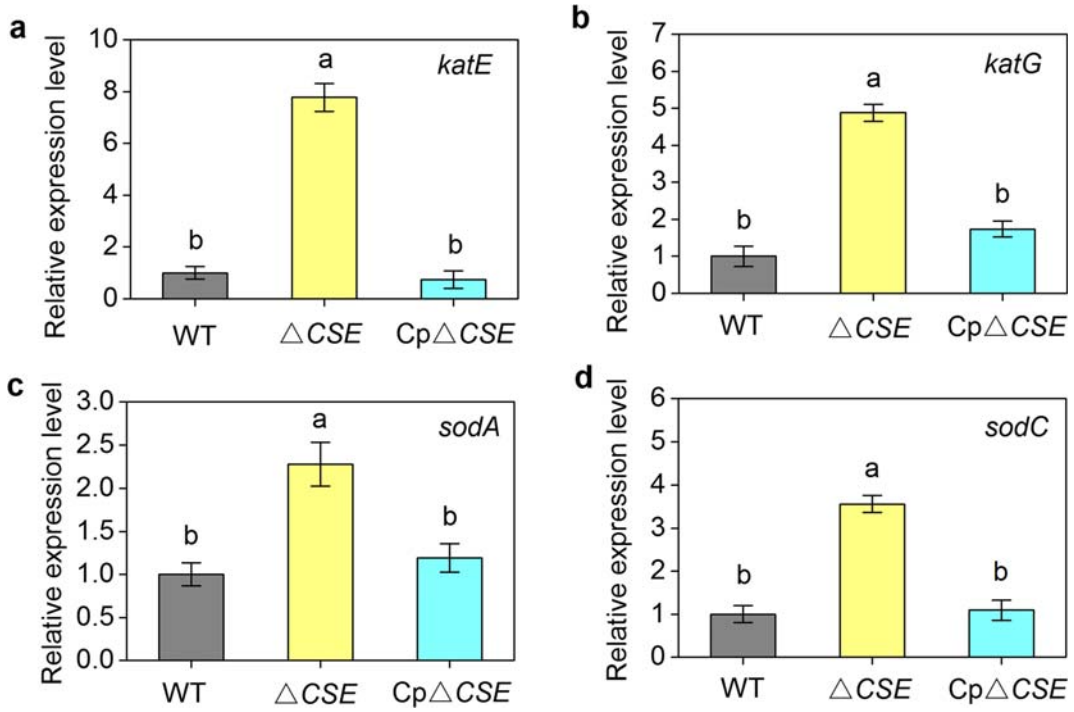

Fig. 8 Relative expression of antioxidant defense genes in bacteroids. (**a**) *katE*; (**b**) *katG*; (**c**) *sodA*; and (**d**) *sodC*. Error bars represent standard error (SE). Values stand for means ± SE of three independent experiments, $n = 9$. The expression level of each gene in Δ*CSE* nodules was relative to the same gene in WT nodules. The mRNA abundances were normalized with that of the endogenous control *16S* ribosomal RNA gene and *rpoD* gene. Different letters above columns indicate significant differences ($P < 0.05$)

Moreover, the expression levels of *GmPrx* and *GmGrx*, which encode 1-Cys peroxiredoxin and glutaredoxin soybean plants, respectively, were significantly higher in Δ*CSE* nodules than in WT nodules (Fig. 9d and e).

Altogether, the up-regulated expression of these antioxidant elements in both the rhizobial symbiont and the plant host suggests that the impaired production of H_2S could cause an antioxidant defense reaction in soybean nodules.

Impaired H_2S generation alters antioxidant-related enzymatic activities and antioxidant content in nodules

As the low production of H_2S led to up-regulated the expression of several antioxidant genes in soybean root nodules, we examined the activity of some crucial antioxidant enzymes in nodules. The activities of SOD and CAT were significantly increased in Δ*CSE* nodules compared to WT and Cp△*CSE* nodules (Fig. 10a and b). Additionally, diminished H_2S in Δ*CSE* nodules resulted in the impaired activity of thioredoxin reductase (TrxR, Fig. 10c). Besides, the SOD and CAT activity within isolated bacteroids and nodule homogenate without bacteroids were also provoked by the deletion of CSE (Fig. S2). This result is similar to that of MDA and protein carbonyl content assay, and also indicated that H_2S deficit could cause antioxidant response to both bacteroids and plant cells.

Also, as a potential element of the antioxidant system, H_2S also influenced the content of other antioxidants in root nodules. In Δ*CSE* nodules, the content of two well-known antioxidants, reduced glutathione (GSH) and NADP(H), were strongly reduced (Fig. 11a, b). Moreover, the H_2S level in soybean root nodules has a significant effect on the content of the sulfhydryl group. According to our results, the H_2S deficit in Δ*CSE* nodules significantly reduced the total thiol content (Fig. 11c).

Discussion

H_2S is required for maintaining symbiotic N fixation in soybean root nodules

Since H_2S became a focal point in plant physiology, many studies have revealed its regulatory effects in

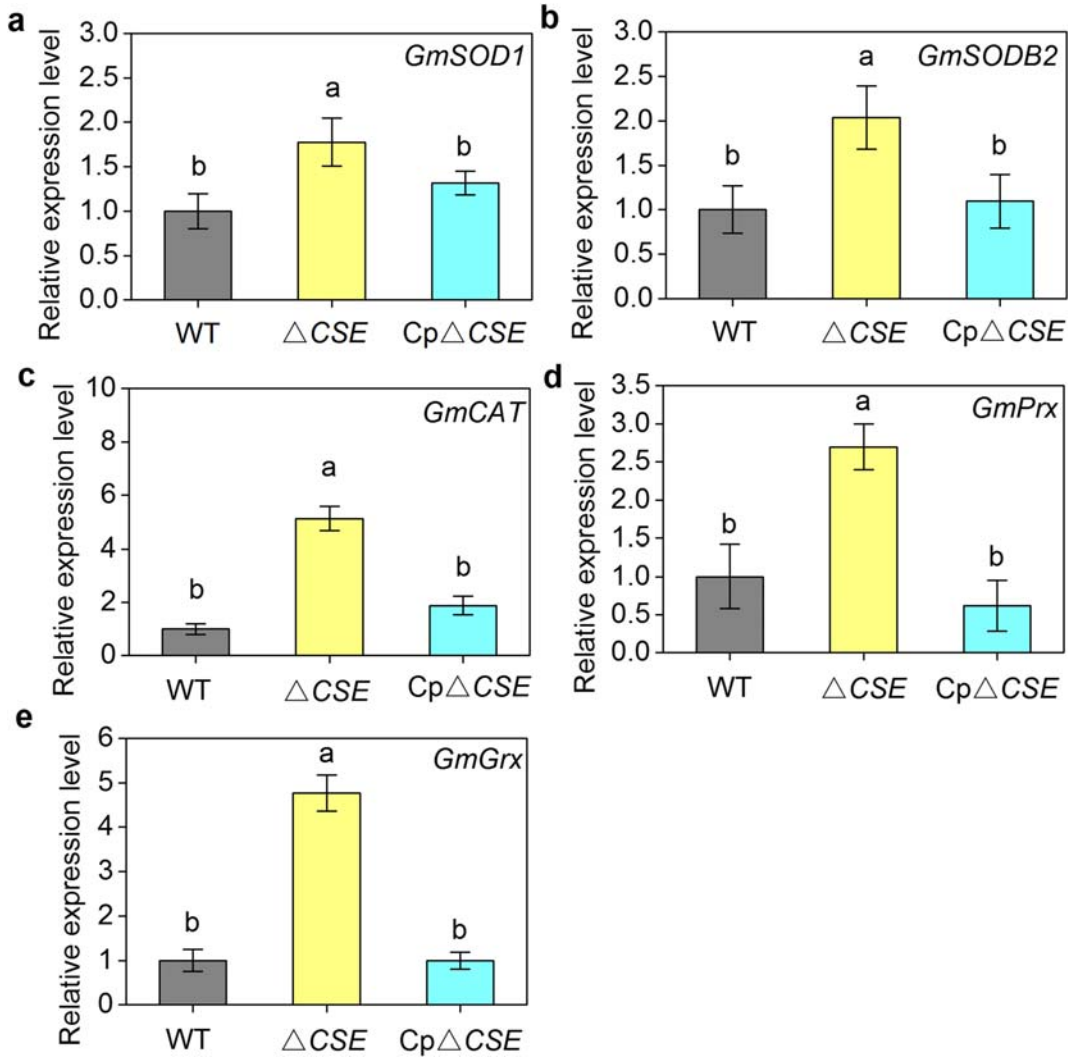

Fig. 9 Relative expression of soybean antioxidant defense genes. (**a**) *GmSOD1*; (**b**), *GmSODB2*; (**c**) *GmCAT*; (**d**) *GmPrx*; and (**e**) *GmGrx*. Error bars represent standard error (SE), values stand for means ± SE of three independent experiments, n = 9. The expression level of each gene in Δ*CSE* and CpΔ*CSE* nodules was relative to the same gene in WT nodules. The mRNA abundances were normalized with that of the endogenous control gene *GmTUB, GmEIF1B and Gmactin*. Different letters indicate significant differences ($P < 0.05$)

plants as a signaling module. For example, H_2S has positive effects in many plant physiological processes such as promoting root organogenesis in soybean (Zhang et al. 2009), enhancing photosynthesis in spinach (*Spinacia oleracea*) (Chen et al. 2011), and alleviating iron deficiency in maize (*Zea mays*) (Chen et al. 2015). Our research has additionally provided a new perspective that H_2S may function as a positive regulator of N fixation in the symbiosis between soybean and *S. fredii*. In this case, the presence as well as the optimal content of H_2S is important for the performance of soybean nodules in symbiotic N fixation.

In the present study, we observed substantial H_2S production in mature soybean root nodules using the fluorescent probe SF7-AM. This probe is reported to be cell-permeable and specifically react with H_2S to form green fluorescence (Lin et al. 2013). We found that the production of H_2S was restricted to the N-fixing zone, where the nodule cells were infected by rhizobia (Fig. l). According to Chrysanthi et al. (2015), N-fixing nodules are rich in thiol and cysteine, and so together with the high metabolic rate, H_2S production in root nodules could be involuntary. They also stated that sulfur assimilation and metabolism were dampened in non-

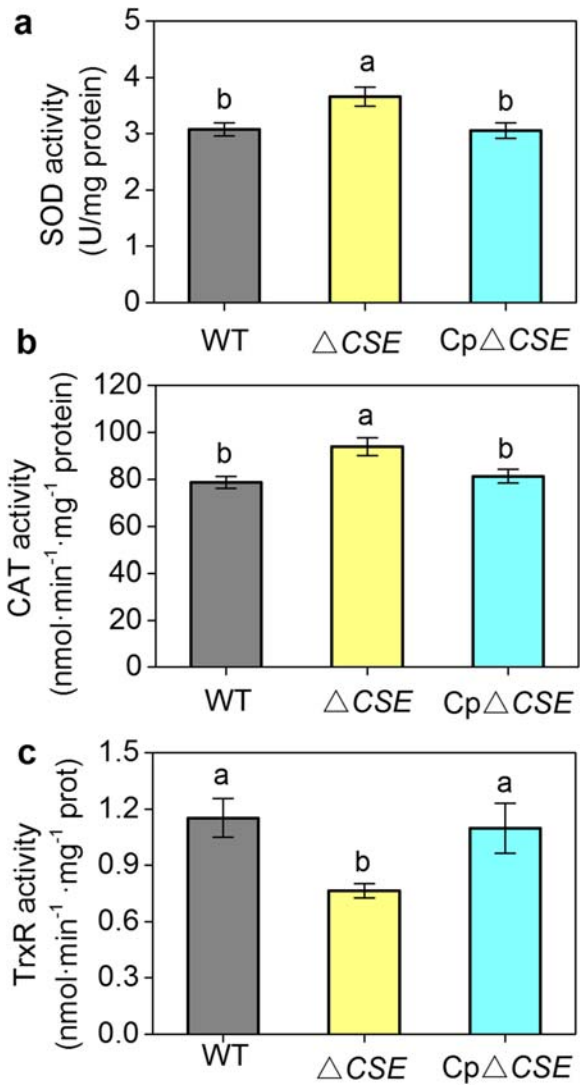

Fig. 10 Antioxidant enzyme activities in WT, Δ*CSE*, and CpΔ*CSE* nodules. (**a**) Superoxide dismutase (SOD); (**b**) Catalase (CAT); and (**c**) Thioredoxin reductase (TrxR). Error bars represent standard error (SE). Values stand for means ± SE of three independent experiments, $n = 15$. Different letters above the columns indicate significant differences ($P < 0.05$)

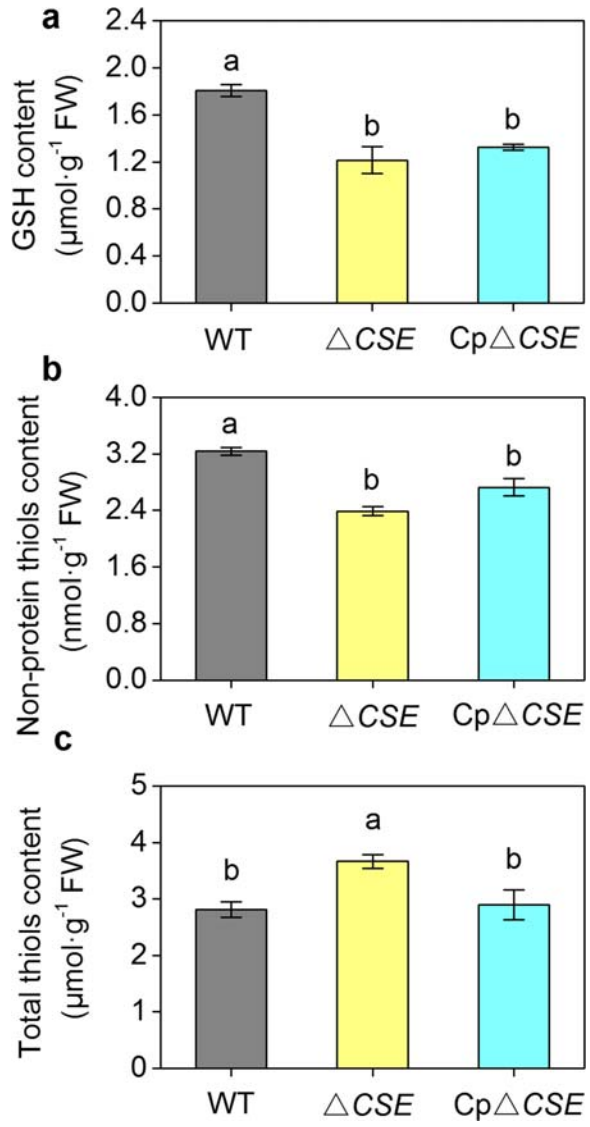

Fig. 11 GSH, NADP(H) and total thiols content determination. (**a**) GSH content in soybean nodules; (**b**) NADP(H) content in soybean nodules; (**c**) Total thiols content in soybean nodules. Error bars represent standard error (SE). Values stand for means ± SE of three independent experiments, $n = 15$. Different letters above the columns indicate significant differences ($P < 0.05$)

inoculated *L. japonicus* or in the plants nodulated by non-nitrogen-fixing (Fix^-) mutant rhizobia. Taken together with our observation, we postulated that the production of H_2S may be coupled with N fixation in soybean nodules.

To verify the coupling of H_2S and N fixation, we constructed a *CSE* knockout *S. fredii* mutant. It has been reported that CSE is the main source of endogenous H_2S in many species of bacteria (Shatalin et al. 2011; Wu et al. 2015). Herein, the Δ*CSE* mutant exhibited significantly impaired H_2S content in both TY medium and soybean root nodules (Fig. 2). Moreover, the previous study has suggested that both the plants and the rhizobial partners can generate H_2S using their own enzymatic systems (Rausch and Wachter 2005). In the present study, the knockout of *CSE* caused more than 75% loss of H_2S production in the free-living *S. fredii* (Fig. 2a), which is much higher than the 48% loss of H_2S content in soybean nodules (Fig. 2b). This

discrepancy in H_2S production between free-living and symbiotic conditions implies that while bacteroids are a major source of H_2S in soybean nodule cells, the plant also contributes to H_2S production. The result of ARA and N content determination suggested that there is a significant correlation between H_2S content and N fixation in soybean nodules (Figs. 3, 4). Our recent study investigated that exogenous H_2S treatment can effectively promote the activity of Nase in soybean nodules (Zou et al. 2019). Similarly, in the present study, the Nase activity partially recovered in Δ*CSE* nodules after the NaHS pretreatment. Conversely, the HT pretreatment led to loss of Nase activity in WT soybean nodules. Thus, the use of NaHS and HT confirmed that the variation in Nase activity was due to the different H_2S content in the soybean nodules. Altogether, our results indicating that H_2S may play an important role in maintaining N fixation in soybean root nodules.

H_2S protects nodule cells and bacteroids from oxidative damage

Due to their high oxidizing capacity, ROS are ubiquitously dangerous in plant cells. High levels of ROS may cause several types of damage to bioactive molecules (Møller et al. 2007; Dietz 2010). Thus, plant cells have evolved specific mechanisms to tightly control the generation and detoxification of ROS. In N-fixing root nodules, many processes, including N fixation, can generate ROS (Becana et al. 2001). The high rate of respiration required to fulfill the intensive energy demand for N fixation in root nodules can generate ROS during electron transfer. Additionally, many O_2-labile proteins and reducing compounds can react with O_2 and readily generate ROS. Thus, the antioxidant defense is especially crucial for root nodules (Becana et al. 2010). It has been reported that H_2S is an essential antioxidant element against ROS and oxidative damage caused by antibiotics in many pathogenic bacteria and the model bacteria *E. coli* (Shatalin et al. 2011; Mironov et al. 2017). In the present study, through TEM observation, we found structural changes in nodule cells which are very similar to those observed in nodules that were senescent or suffering from abiotic stresses (Balestrasse et al. 2004; Li et al. 2008). It is worth noting that under both senescence and heavy metal stress conditions, ROS were reported to be generated in plant tissues and to be responsible for the oxidative damage (Evans et al. 1999; Finkel and Holbrook 2000; Sandalio et al. 2009). To further explore the relevance of H_2S and ROS, we observed the distribution of H_2O_2 in soybean nodules. H_2O_2 is the most common ROS that is generated during symbiosis. Except for its signaling function in the early stage the symbiosis (Cardenas et al. 2008; Santos et al. 2001), H_2O_2 was related to programmed cell death and degradation of the symbiosome in soybean nodules (Alesandrini et al. 2003; Rubio et al. 2004). Beyond that, H_2O_2 could generate hydroxyl radicals by participating in the well-known Fenton reaction and cause severe oxidative damage. As shown in Fig. 6, H_2S significantly reduced the generation and accumulation of H_2O_2 in soybean nodules. This result consists with the finding by Santos et al. (2001) and Rubio et al. (2004). In the context of our study, the fact that the deletion of *CSE* led to a significant increase in H_2O_2 content, may have indicated that H_2S helps in controlling the H_2O_2 level in soybean nodules.

Further proof was provided by the assay of oxidative damage parameters in root nodule tissues. We found that in Δ*CSE* nodule, the protein carbonyl content was significantly higher, which may have indicated a higher level of protein oxidation damage (Romero-Puertas et al. 2002). Besides, as suggested by Shulaev and Oliver (2006), MDA, an end product of lipid peroxidation, is widely accepted as a marker of oxidative damage and has been extensively used in plants. In plant cells, various physiological processes rely on functional membrane system (Gombos et al. 1994). Much of the damage caused by ROS has been reported to be related to membrane lipid peroxidation, such as photosynthetic loss (Galatro et al. 2013), leaf senescence (Dhindsa et al. 1981), and inhibition of root elongation (Yamamoto et al. 2001). Here we found that the MDA content in soybean nodules was significantly higher in Δ*CSE* root nodules than in WT nodules (Fig. 7c). Together with the impaired peribacteroid membrane observed in Δ*CSE* nodules cells by TEM, the MDA assay suggested that lipid peroxidation is more severe without sufficient H_2S. In this regard, the most probable explanation for the increased protein carbonyl content, MDA content and deformed bacteroids is that due to the decreased antioxidant activity by H_2S, the ROS level was elevated and eventually led to the protein oxidation, lipid peroxidation, and deformation of symbiosome membranes in the soybean nodule cells. Moreover, the diminished H_2S level also resulted in a sharp decrease in O_2^- scavenging capacity in Δ*CSE* nodules. Furthermore, MDA and protein carbonyl content determination

in isolated bacteroids and nodule homogenate without bacteroids suggested that H2S deficit in nodules could cause oxidative damage to both bacteroids and plant cells in soybean nodule (Fig. S1). Altogether, our data provide solid proof that H_2S may function as a ROS detoxifier in soybean nodules during symbiotic N fixation.

Deficient H_2S production induces responses of the antioxidant-related enzymatic system

The qRT-PCR data revealed that the disrupted H_2S production in Δ*CSE* nodules stimulated the expression of antioxidant genes (Figs. 8 and 9). On the rhizobial side, oxidative stress in root nodules may lead to the up-regulation of defense and signaling-related gene expression (Mouradi et al. 2018). Impaired carbon metabolism and loss of N-fixation ability are also found in nodules under oxidative stress (Naya et al. 2007; Ramirez et al. 2016). In the rhizobium *Mesorhizobium loti*, *katE* encodes a monofunctional CAT, which is responsible for H_2O_2 detoxification under symbiotic conditions. A *katE* knockout *M. loti* strain has been shown to form nodules with significant loss of N-fixation ability (Hanyu et al. 2009). As for *katG*, it has been related to H_2O_2 detoxification under free-living conditions in *Bradyrhizobium japonicum* (Vargas et al. 2003; Panek and O'Brian 2004). In root nodules, rhizobial *sodA* and *sodC* have been suggested to encode SOD of different isoforms. Iron or manganese could be utilized by SodA as cofactors, while sodC uses copper or zinc as cofactors (Becana and Salin 1989). Our present study identified that bacteroids in H_2S-deficient Δ*CSE* nodules exhibited elevated transcription levels of the *katE*, *katG*, *sodA*, and *sodC* genes (Fig. 8). Similarly, the transcript abundance of several plant genes related to antioxidant defense also increased in the Δ*CSE* nodules (Fig. 9). In Δ*CSE* nodules, *GmSOD1* and *GmSODB2*, which encode the copper/zinc SOD and iron-SODB2, exhibited higher expression levels than in WT nodules. Moreover, the mRNA abundance of 1-Cys peroxiredoxin and glutaredoxin which are encoded by *GmPrx* and *GmGrx* are higher in Δ*CSE* nodules. Herbette et al. (2002) and Groten et al. (2006) found that peroxiredoxin and glutaredoxin may catalyze the conversion of H_2O_2 or alkyl hydroperoxides to water or corresponding alcohols in pea nodules and tomato leaves. The up-regulation of antioxidant gene expression is usually related to abiotic stresses that cause oxidative damage in plant cells (Chen et al. 1993; Borsani et al. 2001; Pekker et al. 2002; Ribera-Fonseca et al. 2013). Thus, our result implied that the H_2S deficit provoked antioxidant defense responses in soybean nodules.

According to the results of the enzymatic activity assay, the activities of some key enzymes (i.e., SOD and CAT) related to antioxidant defense were significantly high in Δ*CSE* nodules (Fig. 10). Besides, SOD and CAT activity determination were also conducted by isolated bacteroids and nodule homogenate without bacteroids. The results suggested that SOD and CAT in both bacteroids and plant cells was up-regulated (Fig. S2). A plausible explanation is that the deletion mutation in the *CSE* gene in bacteroids, which led to significantly decreased antioxidative H_2S content in soybean root nodules. To maintain the redox balance, the activities of SOD and CAT were elevated to compensate for the loss of H_2S production in soybean nodules. On the other hand, the activity of TrxR was strongly inhibited in Δ*CSE* nodules (Fig. 10). It has been reported that thioredoxins are crucial element involved in the regulation of the development of soybean root nodules and they play a vital role in eliminating ROS in soybean root nodules (Lee et al. 2005). TrxR is an enzyme that can reduce oxidized thioredoxins, which is important for maintaining their antioxidant function (Frendo et al. 2013). In the present study, insufficient H_2S production strongly inhibited the activity of TrxR. This could cause further oxidative damage to the N-fixation processes in nodule cells.

Mechanism of H_2S's antioxidant effect

Here, our study evaluated the antioxidant effect of H_2S in soybean root nodules. However, the mechanism underlying still needs further explanation. Our results showed that one of the direct mechanisms that H_2S could influence the redox environment is that H_2S level in soybean root nodules could significantly change the content of GSH and NADP(H) in soybean root nodules. Previous studies demonstrated that GSH plays a crucial part in the antioxidant regulation in soybean root nodules through an ascorbate-GSH cycle which results ultimately in the detoxification of H_2O_2 at the expense of NADP(H) (Dalton et al. 1992; Dalton et al. 1986). Moreover, Chen et al. (2011) reported that H_2S may lead to the accumulation of GSH in plant tissues. Our result also demonstrated that H_2S in soybean nodules could maintain the content of two key elements in the

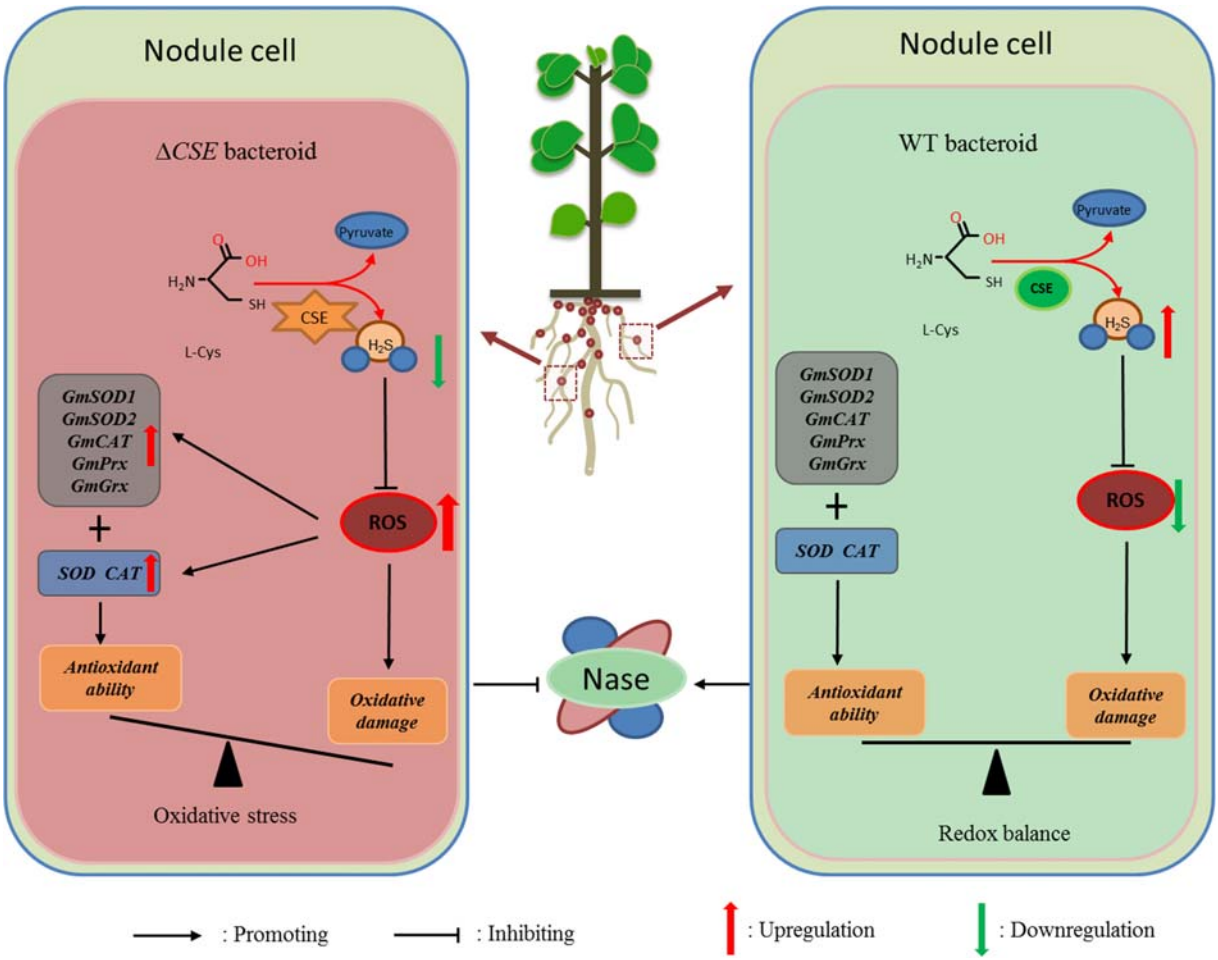

Fig. 12 A schematic model of the mechanisms underlying the antioxidant role of H_2S in the *G. max–S. fredii* symbiotic root nodules

ascorbate-GSH cycle (Fig. 11a, b). This may also help to explain the antioxidant effect of H_2S in the present study that H_2S could help keep the redox balance in soybean root nodules by maintaining the GSH and NADP(H) content.

On the other hand, Aroca et al. (2018) suggested that H_2S may act as a molecular switch by a posttranscriptional modification (PTM) pathway known as persulfidation. This persulfidation modification mainly takes place on the thiol (-SH) of cysteine residue in proteins and thereby changes enzyme activities, structures and cellular localization (Aroca et al. 2015; Aroca et al. 2017b). Among the identified persulfided proteins, ascorbate peroxidase (APX) is a key element involved in peroxide scavenging through the ascorbate-GSH cycle. Aroca et al. (2015) reported that persulfidation modification by H_2S could strongly up-regulate the APX activity in *Arabidopsis thaliana*. In the present study, our result found that total thiol content was altered in Δ*CSE* nodules (Fig. 11c). This result may have indicated that persulfidation level was affected by H_2S. With a deeper meaning that H_2S could regulate the redox environment in soybean nodules through persulfidation modification.

Conclusion

In this study, we investigated that H_2S was generated in the N-fixing zone of soybean root nodules. Deficient H_2S production in soybean nodules led to the accumulation of H_2O_2, which resulted in oxidative damage to bacteroids and the Nase complex. Additionally, the deficit of H_2S triggered antioxidant defense responses in soybean root nodules, including altered antioxidant content, enhanced activity of antioxidant enzymes and up-

regulated expression of antioxidant genes (Fig. 12). Altogether, the results provide evidence that H_2S may play a role in optimizing N fixation in soybean root nodules by acting as an antioxidant element.

Acknowledgments We are grateful for the kind help provided by Yan-Qing Wang and Ke-Rang Huang for microscopy analysis. This work was supported by the Natural Science Foundationof China (31501822 and 41830755) and the Postdoctoral Science Foundation of China (2015 M580876 and 2016 T90948).

References

Afendra AS, Drainas C (1987) Expression and stability of a recombinant plasmid in *Zymomonas mobilis* and *Escherichia coli*. J Gen Microbiol 133:127–134

Alesandrini F, Mathis R, Van de Sype G, Herouart D, Puppo A (2003) Possible roles for a cysteine protease and hydrogen peroxide in soybean nodule development and senescence. New Phytol 158:131–138

Alvarez C, Calo L, Romero LC, García I, Gotor C (2010) An O-acetylserine(thiol)lyase homolog with L-cysteine desulfhydrase activity regulates cysteine homeostasis in *Arabidopsis*. Plant Physiol 152:656–669

Alvarez C, Garcia I, Moreno I, Esther Perez-Perez M, Crespo JL, Romero LC, Gotor C (2012) Cysteine-generated sulfide in the cytosol negatively regulates autophagy and modulates the transcriptional profile in Arabidopsis. Plant Cell 24:4621–4634

Aravind P, Prasad MNV (2005) Modulation of cadmium-induced oxidative stress in *Ceratophyllum demersum* by zinc involves ascorbate-glutathione cycle and glutathione metabolism. Plant Physiol Biochem 43:107–116

Aroca A, Serna A, Gotor C, Romero LC (2015) S-sulfhydration: a cysteine posttranslational modification in plant systems. Plant Physiol 168:334–342

Aroca A, Benito JM, Gotor C, Romero LC, Kopriva S (2017a) Persulfidation proteome reveals the regulation of protein function by hydrogen sulfide in diverse biological processes in *Arabidopsis*. J Exp Bot 68:4915–4927

Aroca A, Schneider M, Scheibe R, Gotor C, Romero LC (2017b) Hydrogen sulfide regulates the cytosolic/nuclear partitioning of Glyceraldehyde-3-phosphate dehydrogenase by enhancing its nuclear localization. Plant Cell Physiol 58:983–992

Aroca A, Gotor C, Romero LC (2018) Hydrogen sulfide signaling in plants: emerging roles of protein Persulfidation. Front Plant Sci 9:1621–1633

Balestrasse KB, Gallego SM, Tomaro ML (2004) Cadmium-induced senescence in nodules of soybean (*Glycine max L.*) plants. Plant Soil 262:373–381

Becana M, Salin ML (1989) Superoxide dismutases in nodules of leguminous plants. Can J Bot 67:415–421

Becana M, Dalton DA, Moran JF, Iturbe OI, Matamoros MA, Rubio MC (2001) Reactive oxygen species and antioxidants in legume nodules. Physiol Plant 109:372–381

Becana M, Matamoros MA, Udvardi M, Dalton DA (2010) Recent insights into antioxidant defenses of legume root nodules. New Phytol 188:960–976

Borsani O, Diaz P, Agius MF, Valpuesta V, Monza J (2001) Water stress generates an oxidative stress through the induction of a specific cu/Zn superoxide dismutase in *Lotus* corniculatus leaves. Plant Sci 161:757–763

Cardenas L, Martinez A, Sanchez F, Quinto C (2008) Fast, transient and specific intracellular ROS changes in living root hair cells responding to nod factors (NFs). Plant J 56:802–813

Chen ZX, Silva H, Klessig DF (1993) Active oxygen species in the induction of plant systemic qcquired-resistance by slicylic-acid. Science 262:1883–1886

Chen J, Wu FH, Wang WH, Zheng CJ, Lin GH, Dong XJ, He JX, Pei ZM, Zheng HL (2011) Hydrogen sulphide enhances photosynthesis through promoting chloroplast biogenesis, photosynthetic enzyme expression, and thiol redox modification in *Spinacia oleracea* seedlings. J Exp Bot 62:4481–4493

Chen J, Wu FH, Shang YT, Wang WH, Hu WJ, Simon M, Liu X, Shangguan ZP, Zheng HL (2015) Hydrogen sulphide improves adaptation of Zea mays seedlings to iron deficiency. J Exp Bot 66:6605–6622

Chen J, Shang YT, Wang WH, Chen XY, He EM, Zheng HL, Shangguan ZP (2016) Hydrogen sulfide-mediated polyamines and sugar changes are involved in hydrogen sulfide-induced drought tolerance in *Spinacia oleracea* seedlings. Front Plant Sci 7:543–551

Cheng W, Zhang L, Jiao C, Su M, Yang T, Zhou L, Peng RY, Wang RR, Wang CY (2013) Hydrogen sulfide alleviates hypoxia-induced root tip death in *Pisum sativum*. Plant Physiol Biochem 70:278–286

Chrysanthi K, Panagiotis K, Georgios K, Udvardi MK, Heinz R, Cornelia H, Emmanouil F (2015) Nitrogen-fixing nodules are an important source of reduced sulfur, which triggers global changes in sulfur metabolism in Lotus japonicus. Plant Cell 27:2384–2400

Dalton DA (1995) Antioxidant defenses of plants and fungi. In: Ahmad S (ed) Oxidative stress and antioxidant defenses in biology. Springer, Boston, pp 298–355

Dalton DA, Russell SA, Hanus F, Pascoe GA, Evans HJ (1986) Enzymatic reactions of ascorbate and glutathione that prevent peroxide damage in soybean root nodules. Proc Natl Acad Sci U S A 83:3811–3815

Dalton DA, Langeberg L, Robbins M (1992) Purification and characterization of monodehydroascorbate reductase from soybean root nodules. Arch Biochem Biophys 292:281–286

Dhindsa RS, Plumb-Dhindsa P, Thorpe TA (1981) Leaf senescence: correlated with increased levels of membrane permeability and lipid peroxidation, and decreased levels of superoxide dismutase and catalase. J Exp Bot 32:93–101

Dickinson BC, Huynh C, Chang CJ (2010) A palette of fluorescent probes with varying emission colors for imaging hydrogen peroxide signaling in living cells. J Am Chem Soc 132:5906–5915

Dietz KJ (2010) Redox-dependent regulation, redox control and oxidative damage in plant cells subjected to abiotic stress. In:

R Sunkar (ed) plant stress tolerance: methods and protocols. Humana press Totowa, pp 57-70

Evans PJ, Gallesi D, Mathieu C, Hernandez NJ, de Felipe N, Halliwell B, Puppo A (1999) Oxidative stress occurs during soybean nodule senescence. Planta 208:73–79

Filipovic MR, Jovanovic VM (2017) More than just an intermediate: hydrogen sulfide signalling in plants. J Exp Bot 68: 4733–4736

Finkel T, Holbrook NJ (2000) Oxidants, oxidative stress and the biology of ageing. Nature 408:239–247

Fishbeck K, Evans HJ, and Boersma LL (1973) Measurement of nitrogenase activity of intact legume symbionts in situ using the acetylene reduction assay. Agron J 65:429–433

Frendo P, Matamoros MA, Alloing G, Becana M (2013) Thiol-based redox signaling in the nitrogen-fixing symbiosis. Front Plant Sci 4:376–385

Galatro A, González PM, Malanga G, Robello E, Piloni NE, Puntarulo S (2013) Nitric oxide and membrane lipid peroxidation in photosynthetic and non-photosynthetic organisms under several stress conditions. Front Physiol 4:276–278

Galton MM, Hess ME (1946) Hydrogen Sulfide Formation by *Shigella alkalescens*. J Bacteriol 52:143–147

Gombos Z, Wada H, Murata N (1994) The recovery of photosynthesis from low-reperature photoinhibition is accelerated by the unsaturation of membrane-lipid-a mechanism fo chilling tollerance. Proc Natl Acad Sci U S A 91:8787–8791

Grosshennig S, Ischebeck T, Gibhardt J, Busse J, Feussner I, Stulke J (2016) Hydrogen sulfide is a novel potential virulence factor of *Mycoplasma pneumoniae*: characterization of the unusual cysteine desulfurase/desulfhydrase HapE. Mol Microbiol 100:42–54

Groten K, Dutilleul C, Heerden PDR, Vanacker H, Bernard S, Finkemeier I, Dietz K-J, Foyer CH (2006) Redox regulation of peroxiredoxin and proteinases by ascorbate and thiols during pea root nodule senescence. FEBS Lett 580:1269–1276

Hanahan D (1983) Studies on transformation of *Escherichia coli* with plasmids. J Mol Biol 166:557–580

Hanyu M, Fujimoto H, Tejima K, Saeki K (2009) Functional differences of two distinct catalases in Mesorhizobium loti MAFF303099 under free-living and symbiotic conditions. J Bacteriol 191:1463–1471

Harrison A, Bakaletz LO, Jr MR (2012) Haemophilus influenzae and oxidative stress. Front Cell Infect Microbiol 2:40–50

Herbette S, Lenne C, Leblanc N, Julien JL, Drevet JR, Roeckel-Drevet P (2002) Two GPX-like proteins from Lycopersicon esculentum and Helianthus annuus are antioxidant enzymes with phospholipid hydroperoxide glutathione peroxidase and thioredoxin peroxidase activities. EJBio 269:2414–2420

Hunt S, Layzell DB (1993) Gas exchange of legume nodules and the regulation of nitrogenase activity. Annu Rev Plant Biol 44:483–511

Kovach ME, Elzer PH, Hill DS, Robertson GT, Farris MA, Ii RMR, Peterson KM (1995) Four new derivatives of the broad-host-range cloning vector pBBR1MCS, carrying different antibiotic-resistance cassettes. Gene 166:175–176

Laureano-Marín AM, Moreno I, Romero LC, Gotor C (2016) Negative regulation of autophagy by sulfide in *Arabidopsis thaliana* is independent of reactive oxygen species. Plant Physiol 171:1378–1391

Lee MY, Shin KH, Kim YK, Suh JY, Gu YY, Kim MR, Hur YS, Son O, Kim JS, Song E, Lee MS, Nam KH, Sung MK, Kim HJ, Chun JY, Park M, Ahn TI, Hong CB, Lee SH, Park HJ, Park JS, Verma DPS, Cheon CI (2005) Induction of thioredoxin is required for nodule development to reduce reactive oxygen species levels in soybean roots. Plant Physiol 139:1881–1889

Li YX, Zhou L, Li YG, Chen DS, Tan XJ, Lei L, Zhou JC (2008) A nodule-specific plant cysteine proteinase, AsNODF32, is involved in nodule senescence and nitrogen fixation activity of the green manure legume Astragalus sinicus. New Phytol 180:185–192

Li L, Wang YQ, Shen WB (2012) Roles of hydrogen sulfide and nitric oxide in the alleviation of cadmium-induced oxidative damage in alfalfa seedling roots. BioMetals 25:617–631

Lin VS, Lippert AR, Chang CJ (2013) Cell-trappable fluorescent probes for endogenous hydrogen sulfide signaling and imaging H_2O_2-dependent H_2S production. Proc Natl Acad Sci U S A 110:7131–7135

Lisjak M, Teklic T, Wilson ID, Whiteman M, Hancock JT (2013) Hydrogen sulfide: environmental factor or signalling molecule? Plant Cell Environ 36:1607–1616

Liu HT, Naismith JH (2008) An efficient one-step site-directed deletion, insertion, single and multiple-site plasmid mutagenesis protocol. BMC Biotechnol 8:91–107

Matamoros MA, Baird LM, Escuredo PR, Dalton DA, Minchin FR, Iturbe-Ormaetxe I, Rubio MC, Moran JF, Gordon AJ, Becana M (1999) Stress-induced legume root nodule senescence. Physiological, biochemical, and structural alterations. Plant Physiol 121:97–112

Matsumura H, Miyachi S (1980) Cycling assay for nicotinamide adenine dinucleotides. Methods Enzymol 69:465–470

Mironov A, Seregina T, Nagornykh M, Luhachack LG, Korolkova N, Lopes LE, Kotova V, Zavilgelsky G, Shakulov R, Shatalin K (2017) Mechanism of H_2S-mediated protection against oxidative stress in *Escherichia coli*. Proc Natl Acad Sci U S A 114:6022

Møller IM, Jensen PE, Hansson A (2007) Oxidative modifications to cellular components in plants. Annu Rev Plant Biol 58: 459–481

Mouradi M, Farissi M, Bouizgaren A, Qaddoury A, Ghoulam C (2018) *Medicago sativa*-rhizobia symbiosis under water deficit: physiological, antioxidant and nutritional responses in nodules and leaves. J Plant Nutr 41:384–395

Naya L, Ladrera R, Ramos J, Gonzalez EM, Arrese-Igor C, Minchin FR, Becana M (2007) The response of carbon metabolism and antioxidant defenses of alfalfa nodules to drought stress and to the subsequent recovery of plants. Plant Physiol 144:1104–1114

Panek HR, O'Brian MR (2004) KatG is the primary detoxifier of hydrogen peroxide produced by aerobic metabolism in Bradyrhizobium japonicum. J Bacteriol 186:7874–7880

Pekker I, Tel-Or E, Mittler R (2002) Reactive oxygen intermediates and glutathione regulate the expression of cytosolic ascorbate peroxidase during iron-mediated oxidative stress in bean. Plant Mol Biol 49:429–438

Peng H, Zhang Y, Palmer LD, Kehl-Fie TE, Skaar EP, Trinidad JC, Giedroc DP (2017) Hydrogen sulfide and reactive sulfur species impact proteome S-sulfhydration and global virulence regulation in *Staphylococcus aureus*. ACS Infect Dis 3:744–755

Qu K, Lee SW, Bian JS, Low CM, Wong PT (2008) Hydrogen sulfide: neurochemistry and neurobiology. Neurochem Int 52:155–165

Ramirez M, Iniguez LP, Guerrero G, Sparvoli F, Hernandez G (2016) *Rhizobium etli* bacteroids engineered for Vitreoscilla hemoglobin expression alleviate oxidative stress in common bean nodules that reprogramme global gene expression. Plant Biotechnol Rep 10:463–474

Rausch T, Wachter A (2005) Sulfur metabolism: a versatile platform for launching defence operations. Trends Plant Sci 10: 503–509

Reibach PH, Mask PL, Streeter JG, (1981) A rapid one-step method for the isolation of bacteroids from root nodules of soybean plants, utilizing self-generating Percoll gradients. Can J Microbiol 27(5):491–495

Redondo FJ, de la Pena TC, Morcillo CN, Lucas MM, Pueyo JJ (2009) Overexpression of flavodoxin in bacteroids induces changes in antioxidant metabolism leading to delayed senescence and starch accumulation in alfalfa root nodules. Plant Physiol 149:1166–1179

Ribera-Fonseca A, Inostroza-Blancheteau C, Cartes P, Rengel Z, Mora ML (2013) Early induction of Fe-SOD gene expression is involved in tolerance to Mn toxicity in perennial ryegrass. Plant Physiol Biochem 73:77–82

Romero-Puertas MC, Palma JM, Gomez M, Del Rio LA, Sandalio LM (2002) Cadmium causes the oxidative modification of proteins in pea plants. Plant Cell Environ 25:677–686

Rubio MC, James EK, Clemente MR, Bucciarelli B, Fedorova M, Vance CP, Becana M (2004) Localization of superoxide dismutases and hydrogen peroxide in legume root nodules. Mol Plant-Microbe Interact 17:1294–1305

Saegesser R, Ghosh R, Bachofen R (1992) Stability of broad host range cloning vectors in the photorophic bacterium *Phodospirillum rubrum*. FEMS Microbiol Lett 95:7–12

Sandalio LM, Rodriguez-Serrano M, del Rio LA, Romero-Puertas MC (2009) Reactive oxygen species and signaling in cadmium toxicity. In: DelRio LA, Puppo A (eds) Reactive oxygen species in plant signaling. Springer, Berlin, pp 175–189

Santos R, Hérouart D, Puppo A, Touati D (2000) Critical protective role of bacterial superoxide dismutase in rhizobium-legume symbiosis. Mol Microbiol 38:750–759

Santos R, Herouart D, Sigaud S, Touati D, Puppo A (2001) Oxidative burst in alfalfa-*Sinorhizobium meliloti* symbiotic interaction. Mol Plant-Microbe Interact 14:86–89

Shatalin K, Shatalina E, Mironov A, Nudler E (2011) H_2S: a universal defense against antibiotics in bacteria. Science 334:986–990

Shi HT, Ye TT, Chan ZL (2013) Exogenous application of hydrogen sulfide donor sodium hydrosulfide enhanced multiple abiotic stress tolerance in bermudagrass (*Cynodon dactylon (L). Pers.*). Plant Physiol Biochem 71:226–234

Shulaev V, Oliver DJ (2006) Metabolic and proteomic markers for oxidative stress. New tools for reactive oxygen species research. Plant Physiol 141:367–372

Soutourina O, Dubrac S, Poupel O, Msadek T, Martin Verstraete I (2010) The pleiotropic CymR regulator of *Staphylococcus aureus* plays an important role in virulence and stress response. PLoS Pathog 6:e1000894

Szabó (2007) Hydrogen sulphide and its therapeutic potential. Nat Rev Drug Discov 6:917–935

Vargas MC, Encarnación S, Dávalos A, Reyes-Pérez A, Mora Y, García-De LSA, Brom S, Mora J (2003) Only one catalase, katG, is detectable in *Rhizobium etli*, and is encoded along with the regulator OxyR on a plasmid replicon. Microbiology 149:1165

Wang R (2002) Two's company, three's a crowd: can H_2S be the third endogenous gaseous transmitter? FASEB J 16:1792–1798

Wang BL, Shi L, Li YX, ZHang WH (2010) Boron toxicity is alleviated by hydrogen sulfide in cucumber (*Cucumis sativus L.*) seedlings. Planta 231:1301–1309

Wu GF, Li N, Mao YT, Zhou GQ, Gao HC (2015) Endogenous generation of hydrogen sulfide and its regulation in *Shewanella oneidensis*. Front Microbiol 6:169–188

Yamamoto Y, Kobayashi Y, Matsumoto H (2001) Lipid peroxidation is an early symptom triggered by aluminum, but not the primary cause of elongation inhibition in pea roots. Plant Physiol 125:199–208

Yang GD, Wu LY, Jiang B, Yang W, Qi JS, Cao K, Meng QH, Mustafa AK, Mu WT, Zhang SM, Snyder SH, Wang R (2008) H_2S as a physiologic vasorelaxant: hypertension in mice with deletion of cystathionine γ-lyase. Science 322: 587–590

Yuan, Z, Zhang Z, Wang X, Li L, Cai K, Han H (2017) Novel impacts of functionalized multi-walled carbon nanotubes in plants: promotion of nodulation and nitrogenase activity in the rhizobium-legume system. Nanoscale 9 (28):9921–9937

Špirić Z, Stafilov T, Vučković I, Glad M (2014) Study of nitrogen pollution in Croatia by moss biomonitoring and Kjeldahl method. J Environ Sci Health A 49 (12):1402–1408

Zhang H, Tang J, Liu XP, Wang Y, Yu W (2008) Hydrogen sulfide promotes root organogenesis in *Ipomoea batatas*, *Salix matsudana* and *Glycine max*. J Integr Plant Biol 51:1086–1094

Zhang H, Tang J, Liu XP, Wang Y, Yu W (2009) Hydrogen sulfide promotes root organogenesis in Ipomoea batatas, Salix matsudana and Glycine max. J Integr Plant Biol 51:1086–1094

Zou H, Zhang N-N, Pan Q, Zhang J-H, Chen J, Wei G-H (2019) Hydrogen sulfide promotes nodulation and nitrogen fixation in soybean–rhizobia symbiotic system.Mol Plant-Microbe Interact 32:972–985